Diversity in the tail of the intersecting brane landscape

JHEP06(2009)073

(http://iopscience.iop.org/1126-6708/2009/06/073)

Published by IOP Publishing for SISSA

Received: *May 19, 2009*
Accepted: *June 5, 2009*
Published: *June 23, 2009*

Diversity in the tail of the intersecting brane landscape

Vladimir Rosenhaus and Washington Taylor

Center for Theoretical Physics, MIT,
Cambridge, MA 02139, U.S.A.

E-mail: vladr@mit.edu, wati@mit.edu

Abstract: Techniques are developed for exploring the complete space of intersecting brane models on an orientifold. The classification of all solutions for the widely-studied $T^6/\mathbb{Z}_2\times\mathbb{Z}_2$ orientifold is made possible by computing all combinations of branes with negative tadpole contributions. This provides the necessary information to systematically and efficiently identify all models in this class with specific characteristics. In particular, all ways in which a desired group G can be realized by a system of intersecting branes can be enumerated in polynomial time. We identify all distinct brane realizations of the gauge groups SU(3) × SU(2) and SU(3) × SU(2) × U(1) which can be embedded in any model which is compatible with the tadpole and SUSY constraints. We compute the distribution of the number of generations of "quarks" and find that 3 is neither suppressed nor particularly enhanced compared to other odd generation numbers. The overall distribution of models is found to have a long tail. Despite disproportionate suppression of models in the tail by K-theory constraints, the tail of the distribution contains much of the diversity of low-energy physics structure.

Keywords: Intersecting branes models, Superstring Vacua

ArXiv ePrint: 0905.1951

doi:10.1088/1126-6708/2009/06/073

JHEP06(2009)073

Contents

1 Introduction

Intersecting Brane Models [1] have been studied for many years as a simple class of string theory constructions giving rise to low-energy physics theories containing a number of desirable features. In particular, these models give rise to low-energy 4-dimensional gauge theories with chiral fermions [2, 3], and have been shown to include supersymmetric models with quasi-realistic phenomenology. For reviews of the subject of intersecting brane

JHEP06(2009)073

models, see [4–10]. Recently, much work has been done on understanding nonperturbative instanton effects in these models, which are relevant for computing Yukawa couplings and for supersymmetry breaking. These developments are reviewed in [11]

In this paper we carry out a detailed analysis of a well-studied class of string compactifications, namely intersecting brane models on the toroidal $T^6/\mathbb{Z}_2 \times \mathbb{Z}_2$ orientifold [12]. These models are computationally very simple, and have been explored extensively. Supersymmetric models have been found in this class with 3 generations of matter in a standard model-like structure [13–18].

The mathematical structure of the vacuum classification problem for intersecting brane models is similar in many ways to that of other string vacuum constructions, such as flux compactifications in type IIB string theory. In all these cases, supersymmetry conditions imply a positive-definite constraint on the topological degrees of freedom encoding the vacuum configuration (i.e. brane windings or fluxes). Topological constraints give a limit to the total tadpole contribution from these combinatorial degrees of freedom, so that the mathematical problem of classifying vacua becomes one of solving a partition problem.

For the intersecting brane models we consider here, this partition problem is complicated by the fact that configurations are allowed in which some tadpoles become negative. These branes with negative tadpoles make even a proof of finiteness of vacuum solutions rather nontrivial. Early work on IBM's on the $T^6/\mathbb{Z}_2 \times \mathbb{Z}_2$ orientifold focused on solutions with certain physical properties. Some systematic analysis of models looking for solutions with standard model-like properties was done in [18]. A systematic computer search through the space of all solutions was carried out in [19, 20]. In some 45 years of computer time (using clusters), 1.66×10^8 consistent models were identified. The results of this analysis suggested that the gauge group and number of generations of various matter fields were essentially independently and fairly broadly distributed, without constraints (up to some upper bounds) in the space of available models, and estimates were given for the frequency of occurrence of various physical features in the models. In [21], the role of branes with negative tadpole contributions ("**A**-branes")[1] was systematically analyzed. It was proven there that the total number of supersymmetric IBM vacuum solutions in this model is finite. Further evidence was given for the broad and independent distributions of gauge group components and numbers of matter fields. Furthermore, analytic tools and estimates were given for numbers of brane configurations with certain properties.

In this paper we complete the program of analysis begun in [21]. We systematically analyze the possible configurations of negative-tadpole **A**-branes which can arise in models of this type. We develop polynomial time algorithms for classifying all **A**-brane configurations, and numerically determine that there are precisely 99,479 such configurations satisfying supersymmetry and tadpole constraints. For each of these **A**-brane configurations, the distribution of remaining branes is given by a partition problem with all branes contributing positive amounts to all tadpoles, so the complete range of models with any desired properties can be carried out in a straightforward fashion given the data on **A**-brane combinations.

[1]Such branes were referred to as "NZ" branes in [18], and "type IV" branes in [28]; we will follow the notation of [21] here, and apologize for confusion due to the variety of prior conventions in the literature.

JHEP06(2009)073

The analysis in this paper is a prototype for other classes of models, such as magnetized brane models on Calabi-Yau manifolds, which may present similar challenges for analyzing vacua due to negative tadpole contributions. The results on **A**-brane configurations enable us to systematically analyze all IBM models on the orbifold of interest with specific physical features. In particular, it is possible to efficiently classify all ways in which a particular gauge group G can appear as a subgroup of the full gauge group. We carry out this analysis for the gauge subgroup $G = \mathrm{SU}(3) \times \mathrm{SU}(2)$, and find some 218,379 distinct ways in which this group G can be realized as a subgroup of the gauge group while satisfying SUSY and undersaturating the tadpole constraints. These constructions can be extended to some 16 million distinct realizations of $\mathrm{SU}(3) \times \mathrm{SU}(2) \times \mathrm{U}(1)$, which we have also enumerated. We look at the number of generations of "quarks" in the (**3, 2**) representation of the gauge group, and find that this generation number generally ranges from 1 to about $\mathcal{O}(10)$, is peaked at 1 and ranges out to 100 or so, with no particular suppression or enhancement of 3 generations relative to other odd generation numbers. In principle all of these constructions of gauge groups of interest can be extended to all complete models containing each realization. K-theory constraints then substantially reduce the number of total possible models.

It is interesting to compare the results of our analysis with those of Gmeiner, Blumenhagen, Honecker, Lüst and Weigand [20]. Those authors carried out a computer scan through models by looking at configurations with small values of toroidal moduli (converted to integers). Their program generated a large class of models arising from constructing all possible combinations of the set of branes compatible with each fixed set of small moduli. While there are many more models for a typical set of small moduli than a typical set of large moduli, we find that the full distribution of models has a very long tail. There are many configurations, particularly those with one or more **A**-branes, which have large values of the (integer-converted) moduli. For these larger moduli, the number of combinatorial possibilities for models is smaller than for small moduli. Nonetheless, there are many distinct moduli for which some models are possible, and the configurations of branes in the tail have a wider range of variability. For example, most of the $\mathrm{SU}(3) \times \mathrm{SU}(2)$ models we have found lie outside the range of moduli scanned in [20]. The long tail of the distribution and the increased diversity of configurations in the tail explain how it is that the computer search by Gmeiner et al. may have covered the region of moduli space containing the greatest total number of models, and nonetheless did not encounter over 95% of the possible ways in which an $\mathrm{SU}(3) \times \mathrm{SU}(2) \times \mathrm{U}(1)$ gauge subgroup can be constructed. In general, we expect the wider diversity of models in the tail to lead to a greater probability of generating models with properties of specific physical interest. So, the answer to a question about "generic" properties of a typical model will depend crucially on how the question is posed. For example if we sample all IBM models which saturate the tadpole conditions and ask for generic properties of random models with given gauge subgroup G, we may get a very different answer than if we sample all distinct ways in which the gauge subgroup G can be realized, independent of the number of other components which can be included in the gauge group through extra branes. Our results suggest in particular that models with a desired gauge group and specific other features (like a particular generation

JHEP06(2009)073

number, no chiral exotic fields, etc.) may be more likely to be found in the "tail" of the distribution than in the "bulk".

The structure of this paper is as follows. In section 2 we review earlier work on intersecting brane models on the toroidal orientifold of interest and define terminology and notation needed for the analysis of the rest of the paper. Section 3 contains a complete analysis of the range of possible **A**-brane configurations. In section 4 we demonstrate how all configurations realizing a desired gauge subgroup G can be enumerated in polynomial time, and give the results of such an enumeration for $G = \mathrm{SU}(3) \times \mathrm{SU}(2)$ and $\mathrm{SU}(3) \times \mathrm{SU}(2) \times \mathrm{U}(1)$. Section 5 contains a comparison of our results with those of the moduli-based search of [20], and a discussion of the "tail" of the vacuum distribution. We conclude in section 6 with a summary and discussion of further related questions.

2 Review of Intersecting Brane Models

The general structure of intersecting brane models is reviewed in, for example, [7]. We briefly review some of the basic structure of these models relevant for this paper. For the most part we follow the notation and conventions of [7, 21].

2.1 General IBM's

Intersecting brane models are constructed by considering a string compactification on some Calabi-Yau manifold, including branes which can be wrapped around topologically non-trivial cycles in the manifold. The situation of interest here involves supersymmetric configurations of D6-branes wrapped on supersymmetric (special Lagrangian) three-cycles on the Calabi-Yau. Such brane configurations arise when type IIA string theory is compactified on a Calabi-Yau with an orientifold six-plane (O6-plane); the D6-branes are needed in this situation to cancel the negative Ramond-Ramond charge carried by the O6-plane. At points where the branes intersect, there are massless string states giving chiral fermions in the four-dimensional low-energy theory in the uncompactified directions [3].

2.2 $T^6/\mathbb{Z}_2 \times \mathbb{Z}_2$

The specific class of models which we analyze in this paper arise from an orientifold on a particular orbifold limit of a Calabi-Yau. Situations where a singular limit of a Calabi-Yau can be described as a toroidal orbifold are particularly easy to analyze and have long been used as the simplest examples of string compactifications with given amounts of supersymmetry. In this case we consider the toroidal orbifold $T^6/\mathbb{Z}_2 \times \mathbb{Z}_2$. Considering the T^6 as a product of three 2-tori with complex coordinates $z_i, i = 1, 2, 3$, the orbifold group is generated by the actions

$$\rho_1 : (z_1, z_2, z_3) \to (-z_1, -z_2, z_3), \qquad \rho_2 : (z_1, z_2, z_3) \to (-z_1, z_2, -z_3). \tag{2.1}$$

The product of these generators gives an additional element of the orbifold group $\rho_3 = \rho_1\rho_2 : (z_1, z_2, z_3) \to (z_1, -z_2, -z_3)$. The geometric part of the orientifold action is given by

$$\Omega : z_i \to \bar{z}_i \,. \tag{2.2}$$

The symmetry of the T^6 under the orbifold and orientifold actions fixes many of the moduli parameterizing the shape of the torus. Symmetry under the orbifold group guarantees that the torus factorizes as a product of three 2-tori. Symmetry under the orientifold action constrains the complex structure of each torus. For each torus the complex structure $\tau = a + ib$ must map to $\bar{\tau} = a - ib$, which must be in the 2D lattice generated by $(1, \tau)$, so $\tau + \bar{\tau} = 2a$ must be in the lattice. This implies that either $a = 0$ or $a = 1/2$, so that the torus is either rectangular or tilted by one half cycle.

Wrapped branes and tadpoles. Consider first the case where T^6 is the product of three rectangular 2-tori. In this case supersymmetric D6-branes associated with special Lagrangian 3-cycles on the T^6 which are invariant under the orbifold group can be described in terms of winding numbers (n_i, m_i) on the three 2-tori. A brane which cannot be decomposed into multiple copies of a brane with smaller winding numbers has (n_i, m_i) relatively prime for all i, and is known as a *primitive* brane. Each brane has an image under the orientifold action with winding numbers $(n_i, -m_i)$.

There are Ramond-Ramond charges associated with the O6-plane which must be cancelled by the wrapped D6-branes for consistency of the model in the absence of other Ramond-Ramond sources (such as fluxes). Each element ρ in the orbifold group (including the identity) gives rise to an orientifold transformation $\Omega_\rho = \Omega\rho$ which, coupled with world-sheet orientifold reversal, gives a symmetry of the string theory and is associated with an orientifold charge on the fixed plane of Ω_ρ. This gives rise to 4 independent tadpole cancellation conditions, associated with total 6-brane charge along the directions $(x_1x_2x_3), (x_1, y_2, y_3), (y_1, x_2, y_3), (y_1, y_2, x_3)$. Labeling these tadpoles P, Q, R, S, each brane with winding numbers (n_i, m_i) contributes to the tadpoles (with appropriate sign conventions)

$$\begin{aligned} P &= n_1 n_2 n_3 \\ Q &= -n_1 m_2 m_3 \\ R &= -m_1 n_2 m_3 \\ S &= -m_1 m_2 n_3 \,. \end{aligned} \tag{2.3}$$

The cancellation of tadpoles requires that summing over all branes, indexed by a, must give

$$\sum_a P_a = \sum_a Q_a = \sum_a R_a = \sum_a S_a = T = 8 \tag{2.4}$$

where $-T = -8$ is the contribution to each tadpole from the O6-plane.

When giving explicit examples of branes we will generally indicate the brane by the values of the tadpoles, with winding numbers as subscripts, in the form

$$(P, Q, R, S)_{(n_1,m_1;n_2,m_2;n_3,m_3)} = (-1, 1, 1, 1)_{(1,1;1,1;-1,-1)} \tag{2.5}$$

Supersymmetry conditions. Supersymmetry imposes further conditions on the winding numbers of the branes. The three moduli associated with the shapes of the three 2-tori

can be encoded in three positive parameters[2] j, k, l, in terms of which the supersymmetry conditions become

$$m_1 m_2 m_3 - j m_1 n_2 n_3 - k n_1 m_2 n_3 - l n_1 n_2 m_3 = 0 \tag{2.6}$$

and

$$P + \frac{1}{j} Q + \frac{1}{k} R + \frac{1}{l} S > 0 \tag{2.7}$$

for each brane separately, with the same positive values of the moduli j, k, l for all branes. When all tadpoles are nonvanishing, (2.6) can be rewritten as

$$\frac{1}{P} + \frac{j}{Q} + \frac{k}{R} + \frac{l}{S} = 0\,. \tag{2.8}$$

Finally, there is a further discrete constraint from K-theory which states that when we sum over all branes we must have [22]

$$\sum_a m_1^a m_2^a m_3^a \equiv \sum_a m_1^a n_2^a n_3^a \equiv \sum_a n_1^a m_2^a n_3^a \equiv \sum_a n_1^a n_2^a m_3^a \equiv 0 \ (\mathrm{mod}\ 2)\,, \tag{2.9}$$

where n_i^a, m_i^a give the winding numbers of the ath brane on the ith torus. As we will see, this discrete constraint significantly decreases the extreme end of the tail of the distribution of allowed models on the moduli space.

Branes on tilted tori. Now, we return to the case where the torus is tilted, with $\mathrm{Re}\,\tau = 1/2$. Say the ith torus is tilted. In this case, we can define winding numbers $\hat{n}_i, \hat{m}_i$ around generating cycles $[a_i], [b_i]$ of the tilted torus.[3] In terms of these winding numbers, we can define

$$n_i = \hat{n}_i, \qquad \tilde{m}_i = \hat{m}_i + \frac{1}{2}\hat{n}_i \tag{2.10}$$

which represent the number of times the brane winds along the perpendicular x, y axes on the ith torus. The supersymmetry conditions for a brane on a tilted torus are again (2.6), (2.7) in terms of $n_i, \tilde{m}_i$ defined in (2.10). The tadpole conditions on a tilted torus are given by (2.4) where we use $m_i = 2\tilde{m}_i$ on the tilted tori [28]. A difference which arises on the tilted torus is that the range of values allowed for $(n_i, \tilde{m}_i)$ is different from the condition of relatively prime integers imposed on the winding numbers for the rectangular torus. On the tilted torus, the winding numbers $\hat{n}_i, \hat{m}_i$ must be relatively prime integers. Integrality of $\hat{n}_i, \hat{m}_i$ imposes the constraint that on a tilted torus we must have $n_i \equiv 2\tilde{m}_i (\mathrm{mod}\ 2)$. The relative primality constraint on $\hat{n}_i, \hat{m}_i$ becomes the condition that $n_i, 2\tilde{m}_i$ have no common prime factor $p > 2$, while for $p = 2$ we can have n_i and $2\tilde{m}_i$ both even iff $n_i/2$ and $\tilde{m}_i$ are not congruent mod 2. Because of the common form of the tadpole relations, enumeration of branes on tilted tori is closely related to that of branes on rectangular tori, with some minor modifications from the modified relative primality constraint.

[2] These parameters are $j = j_2 j_3, k = j_1 j_3, l = j_1 j_2$ in terms of the (imaginary) toroidal moduli $\tau_k = i/j_k$ for rectangular tori.

[3] Following the conventions of [7], these generating cycles are given on the complex plane by $2\pi(R_1^i + iR_2^i/2), 2\pi i R_2^i$.

JHEP06(2009)073

Model construction. We can now summarize the degrees of freedom and necessary conditions on these degrees of freedom which must be satisfied to construct an intersecting brane model on $T^6/\mathbb{Z}_2 \times \mathbb{Z}_2$. First, we can have anywhere from 0-3 tilted tori, with the remaining tori rectangular. Then, we wrap any number of branes on the tori, described by winding numbers $n_i, m_i, i = 1, 2, 3$ for each brane, subject to the appropriate primitivity conditions for rectangular/tilted tori, so that the total tadpole from the branes is (2.4). The K-theory constraints (2.9) must be satisfied by the total brane configuration. Finally, moduli j, k, l must be chosen so that the supersymmetry conditions (2.6) and (2.7) are satisfied for each brane. Note that in general 3 branes will be sufficient to completely constrain the moduli, which are then rational numbers since the constraint equations are linear with rational coefficients. In some cases with fewer branes or redundant constraint equations, there are one or two remaining unfixed moduli. In these cases we can always choose representative combinations of moduli which are rational, though this choice is not unique.

Symmetries. The $T^6/\mathbb{Z}_2 \times \mathbb{Z}_2$ model has a number of symmetries under which related models should be identified. Permutations of the three tori can give arbitrary permutations on the indices $i = 1, 2, 3$ of the winding pairs (n_i, m_i), and hence the same permutation on the tadpoles Q, R, S and moduli j, k, l. By 90 degree rotations $n_i \to m_i \to -n_i$ on two of the tori, we have a further symmetry under exchange of P with any of the other tadpoles. This extends the symmetry to the full permutation group on the set of 4 tadpoles. (To realize this symmetry on the moduli it is convenient to write the moduli as $j/h, k/h, l/h$, so that h plays a symmetric role to the other moduli. When the original moduli are rational, we can then uniquely choose h, j, k, l to be integers without a common denominator. We will go back and forth freely between these two descriptions in terms of 3 rational or 4 integral moduli.)

There is a further set of symmetries on the winding numbers which do not affect the tadpoles. We can rotate two tori by 180 degrees, changing sign on n_i, m_i for two of the i's. Each brane also has an orientifold image given by negating all m_i's. We will keep only one orientifold copy of each brane, and fix the winding number symmetries as in section 2.2 of [21] by keeping only branes with certain combinations of winding number signs, as described there.

Types of branes. There are three distinct types of branes which are compatible with the supersymmetry conditions. These types are distinguished by the numbers of nonzero tadpoles and the signs of the tadpoles. The allowed brane types are:

A-branes: these branes have 4 nonzero tadpoles, of which one is negative and 3 positive. An example of an **A**-brane is

$$(P, Q, R, S)_{(n_1,m_1;n_2,m_2;n_3,m_3)} = (-1, 1, 2, 2)_{(1,2;1,1;-1,-1)} \,. \tag{2.11}$$

B-branes: these branes have 2 nonzero tadpoles, both positive. An example of a **B**-brane is

$$(P, Q, R, S)_{(n_1,m_1;n_2,m_2;n_3,m_3)} = (1, 0, 0, 1)_{(1,1;1,-1;1,0)} \,. \tag{2.12}$$

C-branes: these branes have only 1 nonzero tadpole, and are wrapped on cycles associated with the O6 charge. An example of a **C**-brane is

$$(P,Q,R,S)_{(n_1,m_1;n_2,m_2;n_3,m_3)} = (1,0,0,0)_{(1,0;1,0;1,0)}\,. \tag{2.13}$$

C-branes are often referred to as "filler" branes in the literature, since they automatically satisfy the SUSY conditions and can be added to any configuration which undersaturates the tadpoles to fill up the total tadpole constraint.

Low-energy gauge groups and matter content. Given a set of branes and moduli satisfying the tadpole, supersymmetry, and K-theory constraints, the gauge group and matter content of the low-energy 4-dimensional field theory arising from the associated compactification of string theory can be determined from the topological structure of the branes.

A set of N identical branes of type **A** or **B** give rise to a U(N) gauge group in the low-energy theory, from the $N \times N$ strings stretching between the branes. A set of N identical type **C** branes, on the other hand, which are coincident with their orientifold images, give rise to a group[4] Sp(N).

Associated with each pair of branes there are matter fields containing chiral fermions associated with strings stretching between the branes. These matter fields transform in the bifundamental of the two gauge groups of the branes. The number of copies (generations) of these comes from the intersection number between the branes. For two branes with winding numbers n_i, m_i and $\check{n}_i, \check{m}_i$, the intersection number is

$$I = \prod_i (n_i \check{m}_i - \check{n}_i m_i)\,. \tag{2.14}$$

Because of the orientifold, there is a distinction between **A** and **B** type branes a, b, which have images $a' \neq a$ and $b' \neq b$ under the action of Ω, and a **C** type brane c, which is taken to itself under the action of Ω. Given two **A**-type branes $a, \hat{a}$, for example, the intersection numbers $I_{a\hat{a}}$ and $I_{a\hat{a}'}$ are distinct, and must be computed separately, corresponding to matter fields in the fundamental and antifundamental representations of the gauge group on the branes $\hat{a}$. The same is true of type **B** branes, but not type **C** branes, which are equal to their orientifold images. Note that on tilted tori, in the intersection formula (2.14), the winding number $\tilde{m}_i$ is used in place of m_i. Note also that for branes a, d of any type the parity of I_{ad} and $I_{ad'}$ are the same, so that the sum $I_{ad} + I_{ad'}$ is always even. This means that if there is a stack of N branes a and 2 branes d of type **A** or **B**, the number of matter fields in the fundamental of SU(N) and the fundamental of SU(2) (which is equivalent to the antifundamental) is even unless there is a tilted torus in at least one dimension.

[4]There are a variety of notations for symplectic groups in the math and physics literature. By Sp(N) we denote the symplectic group of $2N \times 2N$ matrices composing the real compact Lie group whose algebra has Cartan classification C_N, which can be defined as $Sp(N) = \mathrm{U}(2N) \cap Sp(2N, \mathbb{C})$. Note that this group is referred to by some authors as $USp(2N)$, and by some authors (such as in [7]) as $Sp(2N)$.

JHEP06(2009)073

2.3 The space of SUSY IBM models

As reviewed in [7], the first intersecting brane models with chiral matter which were constructed lacked supersymmetry. There are an infinite number of such models, which generally have perturbative or nonperturbative instabilities. In this paper we restrict attention to supersymmetric models, which have a more robust structure.

For the IBM models on the $T^6/\mathbb{Z}_2 \times \mathbb{Z}_2$ orientifold described above, the problem of constructing supersymmetric models amounts to solving a partition problem. If we have a set of branes indexed by a, for each a the tadpoles form a 4-vector of integers (P_a, Q_a, R_a, S_a). The tadpole constraint says that the sum of these vectors must equal the vector $(T, T, T, T) = (8, 8, 8, 8)$ associated with the orientifold charges. If all tadpoles $P_a, \cdots, S_a$ were nonnegative, with each brane having at least one positive tadpole, then the number of solutions of the associated partition problem would obviously be finite, as the number of possible tadpole charges would be at most $8^4 - 1 = 4095$, a subset of which would be described by a nonzero but finite number of winding number configurations, and the maximum total number of branes would be 32. With some branes allowed to have one negative tadpole, however, it is no longer so clear that the number of solutions of the partition problem must be finite, or even that the number of branes in any solution is bounded.

For fixed values of the moduli j, k, l, it is fairly straightforward to demonstrate that the number of solutions is finite [19]. The SUSY inequality (2.7) states that the linear combination of tadpoles $\gamma_a = P_a + Q_a/j + R_a/k + S_a/l$ is positive for every brane. The total of this quantity over all branes must be $T(1+1/j+1/k+1/l)$, and is therefore bounded for fixed moduli. The contribution to γ_a from each brane is bigger than any of the individual contributions from any positive term. To see this, assume for example that $Q_a > 0$, and we will show that $\gamma_a > Q_a/j$. Assume without loss of generality that $P_a = -P < 0$. From the SUSY equality (2.8) we have $k/R_a < 1/P$, so $R_a/k > P$. Recalling that at most one tadpole is negative, we then have $\gamma_a > Q_a/j + R_a/k - P > Q_a/j$. Thus, for fixed moduli, we have bounded each individual positive tadpole contribution. But since each winding number appears in two tadpoles, this bounds all winding numbers. It follows that there are a finite number of different possible branes consistent with the SUSY conditions for fixed moduli j, k, l. There is therefore a minimum required contribution to γ_a, and therefore a maximum number of branes which can be combined in any model saturating the tadpole conditions, proving that there are a finite number of models for fixed moduli.

In [19, 20], the space of solutions was scanned by systematically running through moduli and finding all solutions saturating the tadpole conditions and solving the SUSY and K-theory constraints for each combination of moduli. Writing the moduli as a 4-tuple of integers $\vec{U} = (h, j, k, l)$ as discussed above, they scanned all solutions up to $|\vec{U}| = 12$. This computer analysis produced some 1.66×10^8 SUSY solutions. Their numerical results indicated that the number of models was decreasing fairly quickly as the norm of the moduli vector increased, so that this set of models seemed to represent the bulk of the solution space.

JHEP06(2009)073

In [21], an analytic approach was taken to analyzing the space of SUSY models. In this paper it was demonstrated using the SUSY conditions that even including all possible moduli, the total number of brane configurations giving SUSY models saturating the tadpole condition is finite. Estimates were found for numbers of models with particular brane structure.

In this paper we complete this analysis. The key to constructing all models with some desired structure is to deal with the **A**-branes systematically. In the next section, we describe how all 99,479 distinct **A**-brane combinations which do not over-saturate the tadpole conditions can be constructed. For each of these combinations it is then straightforward, if tedious, to construct all models which complete the tadpole conditions through addition of type **B** and **C** branes.

3 Constructing A-brane configurations

As discussed above, finding all models in which a combination of branes satisfy the SUSY and tadpole conditions for some set of moduli would be straightforward if all branes had only positive tadpoles. In this situation, all tadpoles in each brane would give positive contributions to the tadpole condition. This would give us upper bounds on the winding numbers for all the branes and on the maximum number of branes in a given configuration. This would then allow us to scan over all allowed winding numbers and hence find all possible models, or all models with some particular desired properties.

Since **A**-branes have a negative tadpole, however, the tadpole constraint alone will not give us upper bounds on the winding numbers. In order to obtain such upper bounds we need to use a combination of the tadpole condition and the SUSY condition. Indeed, this approach was used in [21] to prove that the total number of supersymmetric brane configurations satisfying the tadpole condition is finite. The bounds determined in that paper, however, are too coarse to allow a search for all models in any reasonable amount of time. In this section we obtain tighter bounds, and describe how these can be used to implement a systematic search for all allowed **A**-brane combinations. We have carried out such a search, and describe the results here.

The goal of this section is thus the construction of all possible configurations of **A**-branes compatible with the tadpole and SUSY constraints. Having all **A**-brane configurations is a crucial step in performing a complete search for any class of models. In 3.1 we develop analytic bounds on the various combinations of **A**-branes with different negative tadpoles. These bounds are derived using combinations of the tadpole and SUSY conditions in order to place upper bounds on the winding numbers and the maximum number of branes allowed in a configuration. Then in 3.2 we apply these bounds to construct a complete algorithm for generating all **A**-brane configurations. In 3.3 we summarize the results of an exhaustive numerical analysis of all the **A**-brane combinations. In this section we will be working exclusively with **A**-type branes. In the following section we describe how to systematically add **B**- and **C**-branes to form all configurations with desired physical properties.

JHEP06(2009)073

To simplify the discussion we define some notation. We let $[p, q, r, s]$ denote a configuration consisting of p branes with a negative P tadpole, q branes with a negative Q tadpole, r branes with a negative R tadpole and s branes with a negative S tadpole. Through permutations in the ordering, we can always arrange the branes so that the branes with a negative P tadpole are first in the configuration, followed by those with a negative Q tadpole, then R, then S. Within these groupings the negative tadpoles can be canonically ordered in increasing order of magnitude. A subscript a on a tadpole (P_a etc.) will indicate which brane it belongs to. Also, for convenience, in this section we will write all tadpole numbers as the absolute value of the tadpole contribution, and explicitly insert the minus sign when needed. For instance the tadpoles of a brane $a \leq p$ with a negative P tadpole will be written as $(-P_a, Q_a, R_a, S_a)$. In the same manner, whenever we write a winding number n_i or m_i, it will mean the absolute value of the winding number and we will explicitly insert a minus sign when needed. Throughout this section we will work with four integer moduli h, j, k, l for symmetry in the equations. Also, as in section 2, the tadpole bound of 8 is denoted by T.

3.1 Bounds from SUSY and tadpole constraints

We will classify the **A**-brane configurations in terms of how many different types of tadpoles are negative. There will be four cases to consider: $[p, 0, 0, 0]$ which corresponds to only the P tadpole being negative, $[p, q, 0, 0]$ in which the first p branes have a negative P tadpole and the next q branes have a negative Q tadpole, $[p, q, r, 0]$, and $[p, q, r, s]$.

We begin with the simplest case, $[p, 0, 0, 0]$, for which we can immediately derive bounds on the winding numbers. We then derive several general conditions which are useful in proving tight bounds on the winding numbers in the cases $[p, q, 0, 0]$ and $[p, q, r, 0]$. We end this subsection by finding strong bounds for the winding numbers in the case $[p, q, r, s]$. In fact, it turns out that there are no combinations of **A**-branes which include branes with each of the four tadpoles being negative, so there are in fact no allowed combinations of type $[p, q, r, s]$ with $p, q, r, s > 0$. The details of the proof of this statement are given in the appendix. This result, however, makes the analysis of all **A**-brane combinations much easier, since it immediately indicates that there are at most 8 **A**-branes in any combination (since all have positive tadpoles $S_a > 0$, with $\sum_i S_a \leq 8$).

As the simplest case, we now consider the $[p, 0, 0, 0]$ combinations, which contain p branes with tadpoles $(-P_a, Q_a, R_a, S_a), 1 \leq a \leq p$. Since the Q, R, and S tadpoles are each at least 1, and the sums of the Q, R, and S tadpoles must each be less than or equal to T, there can be a maximum of T branes per configuration. More explicitly, each brane has 6 winding numbers n_i, m_i from which the 4 tadpoles are constructed as cubic combinations through (2.3). Each winding number appears in 2 different tadpoles (for example, n_1 appears in the P and Q tadpoles). All 6 winding numbers appear in at least one of the Q, R, or S tadpoles. Since all the negative tadpoles are P, all 6 of the winding numbers for each brane can be bounded from the tadpole constraint applied to the Q, R, and S tadpoles. For instance, the tadpole constraint tells us that the sum of the Q tadpoles is less than or equal to T. Thus, the sum over branes of $n_1 m_2 m_3$ is $\leq T = 8$, which gives a strong upper bound on the winding numbers n_1^a, m_2^a, m_3^a. We can easily enumerate the allowed

$[p,0,0,0]$ combinations by considering all winding numbers for the first brane which give $Q_1, R_1, S_1 \leq T$, then constructing all second branes which give $Q_1 + Q_2 \leq T, \ldots$, and so on up to at most $T = 8$ branes.

The other cases, with more than one type of negative tadpole, require a somewhat more complicated analysis. In the case $[p,0,0,0]$ we did not need to use the SUSY conditions. In the cases where there is more than one different negative tadpole, however, it is not immediately clear how to bound the number of branes in a configuration. The SUSY condition will play an essential role in this constraint. Rather than immediately analyzing the next case, where both P and Q tadpoles can be negative, we will find it useful to first derive several conditions which will be helpful to us for bounding the winding numbers and number of branes in a general configuration.

In the first condition that we derive we consider the subset of branes in the configuration with negative P or Q tadpoles (*i.e.*, the first $p+q$ branes). Among the first $p+q$ branes in any **A**-brane configuration (ordered as described above) there are no negative R or S tadpoles. When considering constructions of the type $[p,q,0,0]$ we can therefore use the tadpole constraints for the R and S tadpoles to bound 5 of the 6 winding numbers. n_1 is the only winding number which is not immediately bounded by the tadpole conditions, since it is the only one that does not appear in the R or S tadpoles. We now determine a bound for these n_1 winding numbers.

First Winding Number Bound (FWNB). Again, we consider the first $p+q$ branes, which are those having only negative P or Q tadpoles. We choose a, b from $a \in \{1, \ldots, p\}$, $b \in \{p+1, \ldots p+q\}$. The SUSY condition (2.8) for brane a states $-\frac{h}{P_a} + \frac{j}{Q_a} + \frac{k}{R_a} + \frac{l}{S_a} = 0$. We must therefore have $-\frac{h}{P_a} + \frac{j}{Q_a} < 0$. Similarly, from the SUSY condition for brane b we get $\frac{h}{P_b} - \frac{j}{Q_b} < 0$. These two conditions together give $\frac{Q_a}{P_a} > \frac{Q_b}{P_b} \;\; \forall a, b$. Let $\lambda = \max_b \left\{\frac{Q_b}{P_b}\right\}$. Then $\frac{Q_a}{P_a} > \lambda \;\; \forall a$ and $\lambda \geq \frac{Q_b}{P_b} \;\; \forall b$. Note that $\lambda = m_2^b m_3^b / n_2^b n_3^b$ for some b, so λ is independent of the winding numbers n_1 for any brane. From the tadpole conditions for P and Q (upon rearranging) we get:

$$(Q_1 - \lambda P_1) + \ldots + (Q_p - \lambda P_p) + (\lambda P_{p+1} - Q_{p+1}) + \ldots + (\lambda P_{p+q} - Q_{p+q}) \leq T(\lambda + 1) \quad (3.1)$$

Since each term in parenthesis is nonnegative, and the terms from the first p branes are positive, we have a bound on the n_1 winding number of each of the branes with negative p, given all the remaining winding numbers n_2, n_3, m_i for each of these branes. By choosing $\lambda = \min_a \left\{\frac{Q_a}{P_a}\right\}$, we can similarly determine a bound on the n_1 winding numbers for the branes with negative Q_b. We will henceforth refer to these bounds on n_1 (3.1) as FWNB for convenience.

The bound (3.1) makes the construction of all configurations of type $[p,q,0,0]$ a straightforward exercise, similar to that described above for combinations of type $[p,0,0,0]$, as we describe in more detail in the following subsection. We can derive another condition which will be useful for cases with 3 or 4 different negative tadpoles. Once again, we look at the subset of branes in which only two types of tadpole are negative, without loss of generality taking these to be the first $p+q$ branes in the configuration where $-P_a, -Q_b$ are the negative tadpoles.

JHEP06(2009)073

Two Column SUSY Bound (TCSB). For any combination of branes, the tadpole conditions for the R and S branes gives

$$\sum \frac{R}{k} + \sum \frac{S}{l} \leq T\left(\frac{1}{k} + \frac{1}{l}\right), \tag{3.2}$$

where when we do not use indices the sum is taken over all branes and the tadpoles (here R and S) have their correct negative or positive values. For a brane of the type $(P_a, Q_a, -R_a, S_a)$ SUSY gives $\frac{h}{P_a} + \frac{j}{Q_a} - \frac{k}{R_a} + \frac{l}{S_a} = 0$. Hence $-\frac{k}{R_a} + \frac{l}{S_a} < 0$, or rearranging,

$$-\frac{R_a}{k} + \frac{S_a}{l} > 0\,. \tag{3.3}$$

Similarly for branes of the form $(P_a, Q_a, R_a, -S_a)$ there is a positive contribution $\frac{R_a}{k} - \frac{S_a}{l} > 0$.

Thus, we have that, even when restricting to just the first $p+q$ branes where both R and S are positive,

$$\sum_{a=1}^{p+q} \frac{R_a}{k} + \sum_{a=1}^{p+q} \frac{S_a}{l} \leq T\left(\frac{1}{k} + \frac{1}{l}\right) \tag{3.4}$$

The relation (3.4) is possible only if

$$\sum_{a=1}^{p+q} R_a \leq T \text{ or } \sum_{a=1}^{p+q} S_a \leq T \tag{3.5}$$

where the inequality is a strict $<$ if there is at least one brane with a negative R or S tadpole.

The Two Column SUSY Bound (TCSB) is (3.5). This result clearly generalizes to considering the subset of branes with any two tadpoles being purely positive, in which case one of the two positive sums must be $\leq T$. As a consequence of the condition (3.5), we gain useful information about configurations with 3 types of negative tadpoles ($[p, q, r, 0]$). In particular, we can show that

The sum of the positive contributions to one of the first three tadpoles is less than 3T (3.6)

To see this, without loss of generality, we let $h = \min\{h, j, k\}$. We have that

$$\sum \frac{P}{h} + \sum \frac{Q}{j} + \sum \frac{R}{k} \leq T\left(\frac{1}{h} + \frac{1}{j} + \frac{1}{k}\right) \tag{3.7}$$

For a brane of the form $(-P_a, Q_a, R_a, S_a)$ there will be a positive contribution to the above sum since $-\frac{P_a}{h} + \frac{Q_a}{j} > 0$, which can be shown in a similar fashion to (3.3) above. From a brane with a tadpole other than P_a that is negative, say $(P_a, -Q_a, R_a, S_a)$, we have $-\frac{Q_a}{j} + \frac{R_a}{k} > 0$, and so $\frac{P_a}{h}$ will contribute less than the total for that brane to the above sum. Hence we get

$$\sum_{a=p+1}^{p+q+r+s} \frac{P_a}{h} < T\left(\frac{1}{h} + \frac{1}{j} + \frac{1}{k}\right) \leq \frac{3T}{h}\,.$$

This proves (3.6)

Along with the TCSB, this condition suffices to give strong bounds on the winding numbers and the number of branes in a $[p,q,r,0]$ configuration. We describe the details of how these bounds are used to determine the range of $[p,q,r,0]$ configurations in the next subsection. Finally, we need to consider the case of $[p,q,r,s]$. It turns out that there are no configurations of this type which are compatible with SUSY and the tadpole conditions with $T=8$ (though such configurations are possible at larger values of T). The full proof that there are no configurations of this type is given in the appendix. Here we just derive a bound on the maximum number of allowed branes.

Suppose we have $[p,q,r,s]$. Without loss of generality, let $s \leq r \leq q \leq p$ and for convenience of notation, we let $a=p,\ b=p+q,\ c=p+q+r,\ d=p+q+r+s$. The sum of the tadpole conditions for R and S gives

$$\sum \frac{R}{k} + \sum \frac{S}{l} \leq T\left(\frac{1}{k}+\frac{1}{l}\right) \tag{3.8}$$

Looking at the left side of this equation, and using relations like (3.3) we have

$$\frac{R_1+\ldots+R_b}{k} + \frac{S_1+\ldots+S_b}{l} + \underbrace{\left(-\frac{R_{b+1}}{k}+\frac{S_{b+1}}{l}\right)}_{>0} + \ldots + \underbrace{\left(\frac{R_d}{k}-\frac{S_d}{l}\right)}_{>0}$$

This is greater than $(p+q)(\frac{1}{k}+\frac{1}{l})$, so if $(p+q) \geq T$ the tadpole condition is violated. So we have found that

$$\textit{For } (p+q) \geq T \textit{ there are no configurations } [p,q,r,s] \tag{3.9}$$

This condition severely limits the number of branes that can be in a configuration. In fact, by various manipulations of the SUSY equations, we can show there are no configurations of the form $[p,q,r,s]$ when $T=8$ (see appendix for details).

3.2 Algorithm

Using the constraints derived in the previous subsection we can construct algorithms whose complexity scales polynomially in T to generate all **A**-brane configurations. We outline such algorithms for the three cases $[p,0,0,0]$, $[p,q,0,0]$, and $[p,q,r,0]$. In each case, the algorithm consists of scanning over all the winding numbers for all the branes in the configuration subject to given bounds. The bounds on the size of the winding numbers and the number of branes in the configuration are obtained by using combinations of the conditions in the previous section. The main challenge in constructing such algorithms is having explicit bounds for all the winding numbers. So the focus of this discussion is on explaining how all winding numbers can be constrained using the results of the previous subsection.

As we saw in 3.1, for $[p,0,0,0]$ we can simply loop over all six winding numbers for each of the branes, all of which are constrained by the tadpole condition. Considering all winding numbers for the first brane, and then subtracting the resulting contributions for Q_1, R_1, S_1 from the tadpole conditions while assuming that $P_1 \geq P_a, a>1$ gives stronger bounds for the winding numbers of the second brane, and so on.

Generating all **A**-brane configurations of the form $[p, q, 0, 0]$ is only slightly more involved. We loop over 5 of the 6 winding numbers for each brane (since all but n_1 are constrained by the tadpole condition). We then loop over n_1 for each brane after bounding it through use of FWNB. For example, let us look at the simplest case of $[1, 1, 0, 0]$. The tadpole condition for the S tadpole gives (recall that in this section we are using n_i, m_i to denote absolute values of winding numbers, with signs put in explicitly)

$$m_1^1 m_2^1 n_3^1 + m_1^2 m_2^2 n_3^2 \leq T, \tag{3.10}$$

and the tadpole condition for the R tadpole gives

$$m_1^1 n_2^1 m_3^1 + m_1^2 n_2^2 m_3^2 \leq T. \tag{3.11}$$

With these two conditions we have bounds on all winding numbers except for n_1^1 and n_1^2. We can therefore easily loop over all these winding numbers. Concretely, this means we have 10 nested loops. In the first loop, we loop over all $m_1^1 < T$, in the second loop we loop over all m_2^1 such that $m_1^1 m_2^1 < T$, and so on. Finally, we have two additional nested loops for n_1^1 and n_1^2. The maximum values for these are obtained from FWNB. For n_1^1 we have the constraint

$$n_1^1 (m_2^1 m_3^1 - \lambda n_2^1 n_3^1) \leq T(\lambda + 1), \tag{3.12}$$

where $\lambda = \frac{m_2^2 n_3^2}{n_2^2 n_3^2}$. And for n_1^2 we have

$$n_1^2 (\lambda n_2^2 n_3^2 - m_2^2 m_3^2) \leq T(\lambda + 1), \tag{3.13}$$

where $\lambda = \frac{m_2^1 n_3^1}{n_2^1 n_3^1}$. The general case of $[p, q, 0, 0]$ is done by a similar application of FWNB.

The case $[p, q, r, 0]$ requires the most work. The idea is to first generate three branes with all different negative tadpoles. For the purpose of this discussion we rearrange the brane ordering so that these branes can be chosen to have tadpoles

$$(-P_1, Q_1, R_1, S_1), \qquad (P_2, -Q_2, R_2, S_2), \qquad (P_3, Q_3, -R_3, S_3)\,. \tag{3.14}$$

Note that further branes may be added to the configuration with negative P, Q, or R tadpoles. However, for any configuration we choose the first brane to be the brane in that configuration with a negative P tadpole which minimizes Q_a/P_a, and the second brane to be the one with a negative Q tadpole which maximizes Q_b/P_b. Once we have chosen the 3 branes (3.14) we solve for the moduli, and then add all further combinations of branes consistent with those moduli and the tadpole constraints.

The first step is generating the first three branes, (3.14). In order to generate these we need constraints on all the winding numbers for these three branes. From the tadpole constraint on the S tadpole, since the total configuration of which (3.14) is a subset has no branes with negative S, we have bounds on the m_1, m_2 and n_3 winding numbers for each of the branes. To find constraints for the other winding numbers we are not allowed to use the tadpole bound condition on the P, Q, or R tadpoles, since the additional branes we may add to complete the configuration can give negative contributions to these tadpoles. We

JHEP06(2009)073

will thus rely on the conditions derived in subsection 3.1 in order to specify upper bounds on the winding numbers.

We begin by using (3.6). Without loss of generality this condition allows us to assume that $R_1 + R_2 < 3T$. Referring back to FWNB, we take $\lambda = Q_2/P_2$ which in (3.1) gives $(Q_1 - \lambda P_1) < T(\lambda + 1)$ to constrain n_1^1. (Note that since brane 2 has the largest value of Q_b/P_b among all negative Q branes, all contributions on the l.h.s. of (3.1) are positive, even when further branes are included in the configuration.)

Next, we take $\lambda = \frac{Q_1}{P_1}$ and in a similar fashion use $(\lambda P_2 - Q_2) < T(\lambda + 1)$ to constrain n_1^2. At this point, the first two branes are completely constrained (meaning that we have explicit upper bounds on all winding numbers for the first two branes in the configuration).

For the third brane, the TCSB (3.5) for the P and Q tadpoles shows that we have that either $P_3 < T$ or $Q_3 < T$. Without loss of generality we take $P_3 < T$. Thus, for the third brane P_3 and S_3 are now constrained. Using SUSY between branes 1 and 3 we get that $\frac{R_1}{P_1} > \frac{R_3}{P_3}$. Thus $R_3 < P_3 \frac{R_1}{P_1}$ and so R_3 is constrained.

We have thus determined upper bounds on all winding numbers for the three branes (3.14). We now move on to the second step, which involves finding the unique set of moduli consistent with supersymmetry for the first three branes. This will then allow us to efficiently add to the first three branes all branes consistent with the moduli. Having three distinct branes in a configuration is a necessary condition to uniquely determine the moduli, but not a sufficient one (the system of three SUSY equations (2.8) for 3 moduli may not have a unique solution). In order to actually be able to solve for the moduli using the three branes (3.14), we need to prove that these three branes give linearly independent constraints on the moduli. Suppose that the constraints are dependent, so that there exist an α, β such that

$$\alpha\left(-\frac{1}{P_1}, \frac{1}{Q_1}, \frac{1}{R_1}, \frac{1}{S_1}\right) + \beta\left(\frac{1}{P_2}, -\frac{1}{Q_2}, \frac{1}{R_2}, \frac{1}{S_2}\right) = \left(\frac{1}{P_3}, \frac{1}{Q_3}, -\frac{1}{R_3}, \frac{1}{S_3}\right) \tag{3.15}$$

From the linear relation on the first element of the vector we see that either $\alpha < 0$ or $\beta > 0$, from the relation on the second element we need $\alpha > 0$ or $\beta < 0$, from the third either $\alpha < 0$ or $\beta < 0$, and from the fourth, $\alpha > 0$ or $\beta > 0$. There are no solutions to this set of sign constraints.

Having uniquely determined the moduli we can efficiently find all branes consistent with this moduli so we can add them to the branes (3.14) in all ways compatible with the total tadpole constraints. In 2.3 we summarized a simple argument showing that there are a finite number of such possible configurations, and that the winding numbers for each brane can be bounded. For example, each brane with negative P tadpole has positive tadpole contributions Q, R, S bounded by

$$\frac{Q}{j}, \frac{R}{k}, \frac{S}{l} < \gamma = -\frac{P}{h} + \frac{Q}{j} + \frac{R}{k} + \frac{S}{l} \leq T\left(\frac{1}{h} + \frac{1}{j} + \frac{1}{k} + \frac{1}{l}\right) \tag{3.16}$$

Similar bounds can be given for branes with positive P tadpole. This bounds all winding numbers on additional branes to be added to (3.14) once the moduli are fixed. Since all

JHEP06(2009)073

n	1	2	3	4	5	6	7	8
Number Configurations	226	30,255	57,651	9,315	1,615	361	55	1

Table 1. Number of configurations with n **A**-branes.

p\q	0	1	2	3
1	226	28560	-	-
2	1695	52761	3286	-
3	857	5048	694	51
4	105	689	170	0
5	9	89	27	0
6	2	12	0	0
7	1	0	0	0
8	1	0	0	0

Table 2. Number of configurations with p **A**-branes with negative P tadpole, q **A**-branes with negative Q tadpole, and no branes with negative R or S tadpole.

branes contribute a positive amount $\gamma_a > 0$ (by (2.7)) to the sum

$$\sum_a \gamma_a \leq T\left(\frac{1}{h}+\frac{1}{j}+\frac{1}{k}+\frac{1}{l}\right) \tag{3.17}$$

we can combine the additional branes at fixed moduli in only a finite number of ways compatible with the tadpole constraints, which are easily enumerated. This gives us a systematic way of constructing all possible **A**-brane configurations of type $[p, q, r, 0]$.

3.3 Results

We have performed a full search for all possible **A**-brane configurations using the algorithm described in the previous subsection. We find a total of 99,479 distinct configurations (with no tilted tori), after removing redundancies from the permutation symmetries on tadpoles and branes. In table 1 we show the distribution of the number of **A**-branes in these configurations. Note that with more than 3 **A**-branes, the number of possible configurations decreases sharply. The configurations computed here are those which satisfy the SUSY constraints for a common set of moduli and which undersaturate the tadpole constraints. As we discuss in the following sections, to form complete models associated with valid string vacua, **B**-branes compatible with the SUSY equations and "filler" **C**-branes must generally be added to any particular **A**-brane configuration to saturate the tadpole constraints, and then K-theory constraints must be checked.

The number of **A**-branes with negative P and Q tadpoles in configurations of types $[p, 0, 0, 0]$ and $[p, q, 0, 0]$ is tabulated in table 2. So, for example, of the 57,651 combinations with 3 **A**-branes, 857 are of type [3, 0, 0, 0], 52,761 are of type [2, 1, 0, 0], and the remaining 4033 are of type [1, 1, 1, 0].

JHEP06(2009)073

While there are only 226 individual **A**-branes which alone satisfy all tadpole constraints, many more distinct individual **A**-branes are possible in combination with other **A**-branes. The number of distinct (up to symmetry) **A**-branes appearing in any configuration is 3259. A simple consequence of the Two Column SUSY Bound (3.5) is that no individual **A**-brane can have more than one tadpole $> T$. It is possible, however, to have an **A**-brane with one large positive tadpole, compensated by a negative tadpole on another brane. The most extreme case of this is realized in a two **A**-brane combination in which one brane has a tadpole $P = 800$

$$(-792, 3, 3, 88)_{(3,1;3,1;-88,-1)} \; + \; (800, 2, 5, -80)_{(2,1;5,1;80,-1)} \, . \tag{3.18}$$

One of the most significant features of the **A**-brane combinations tabulated in table 1 is that

Any combination of **A***-branes has at most one negative total tadpole*

This was proven in [21] for a combination of two **A**-branes but it is straightforward to generalize to any number of **A**-branes. Consider for example the tadpoles P, Q. As in the discussion in 2.3, for every brane with negative $P_a = -P$ we have from the SUSY condition $Q_a/j - P/h > 0$, and for each brane with negative $Q_b = -Q$ we have $-Q/j + P_b/h > 0$. Thus, in the sum over all branes in any configuration we have

$$\sum_a \frac{P_a}{h} + \frac{Q_a}{j} > 0 \tag{3.19}$$

so that only one of the total tadpoles P, Q can be negative. The same holds for any pair so, as stated above, at most one total tadpole can be negative for any combination.

As a consequence of this result, any combination of **A**-branes acts in a similar fashion to a single **A**-brane. Furthermore, when **A**-branes are added, since the individual winding numbers on each brane must be smaller, the maximum achievable negative tadpole decreases quickly as the branes are combined. Thus, a single **A**-brane can achieve the most negative tadpole. Indeed, the single **A**-brane with the most negative tadpole (and no tadpoles $> T$) is

$$(-512, 8, 8, 8)_{(8,1;8,1;-8,1)} \, . \tag{3.20}$$

The combination of two **A**-branes with the most negative total tadpole is

$$2 \times (-64, 4, 4, 4)_{(4,1;4,1;-4,1)} = (-128, 8, 8, 8) \, . \tag{3.21}$$

For three **A**-branes, the most negative total tadpole is -54, and for four **A**-branes the most negative total tadpole is -32. The distribution of the smallest total tadpole for all combinations of 1-4 **A**-branes (with no total tadpoles $> T$) is depicted in figure 1. In each case, the branes are ordered by minimum total tadpole and distributed linearly along the vertical axis.

We thus see that most multiple **A**-brane configurations have similar properties to a single **A**-brane with a minimum tadpole which is fairly small in absolute value. Only for combinations with a small number of **A**-branes are there configurations with substantially

JHEP06(2009)073

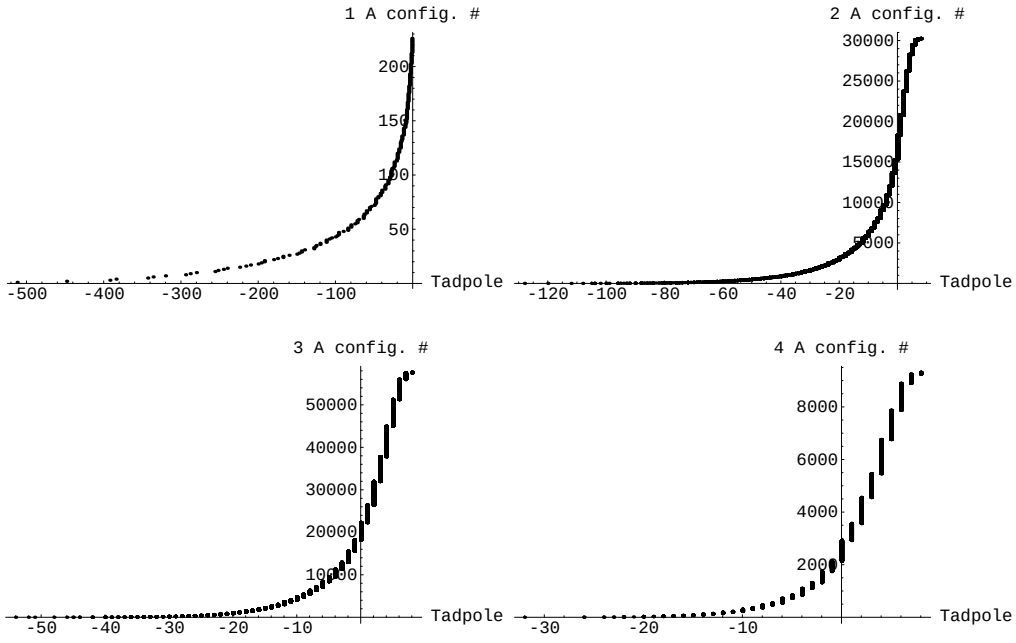

Figure 1. Minimum total tadpole in each configuration of 1, 2, 3, and 4 **A**-branes (untilted tori).

large negative tadpoles. Note, however, that although multiple **A**-brane configurations act similar to a single **A**-brane in terms of the total effect on tadpole contributions, they may act very differently when it comes to satisfying K-theory constraints.

In constructing more general models with multiple stacks of D-branes, the greatest variety of constructions is possible when the smallest total tadpole coming from the **A**-brane sector is as negative as possible. In particular, the greatest flexibility in adding **B**-branes and **C**-branes is afforded when the **A**-brane sector has a very negative total tadpole and the positive total tadpoles are also small. This is realized primarily for single **A**-branes with very negative tadpoles. There are 33 single **A**-branes with negative tadpole ≤ -128, and 71 single **A**-branes with negative tadpole ≤ -54. A typical example is the **A**-brane

$$(-168, 3, 7, 8)_{(3,1;7,1;-8;-1)} \,. \tag{3.22}$$

There are also 403 combinations of two **A**-branes with negative tadpole ≤ -54. The two **A**-brane combinations have larger positive total tadpoles than the single brane configurations with similar negative tadpole, so that the single brane gives space for a wider variety of added **B**- and **C**-branes. As we shall see, most of the diversity of models with multiple brane stacks comes from these single (and some double) brane configurations with highly negative tadpoles. These configurations are also associated with relatively large integer moduli h, j, k, l, as we discuss in more detail in section 5. On the other hand, as we discuss in section 4.5, the K-theory constraints become more restrictive for single **A**-branes with very large negative tadpoles. This effect mitigates to some extent the role of the single **A**-branes with extremely negative tadpoles in generating diversity in constructions of interesting physics models.

JHEP06(2009)073

# tilted tori\n	1	2	3	4	5	6	7	8
1	242	24783	27712	10068	1375	477	36	1
2	136	5897	4868	3127	422	222	9	0
3	29	471	277	354	38	36	0	0

Table 3. Number of configurations of n **A**-branes having all total tadpoles $\leq T = 8$ with 1, 2, or 3 tilted tori.

Finally, we discuss the question of **A**-brane combinations with tilted tori. As described in section 2.2, on a tilted torus the tadpole and winding number conditions are very similar to those on a rectangular torus, but the winding numbers on the tilted torus must satisfy $n_i \equiv 2\tilde{m}_i \pmod 2$. The relative primality condition is weakened so that n_i and $2\tilde{m}_i$ can both be even, if $n_i/2 \not\equiv \tilde{m}_i \pmod 2$. We can realize all brane combinations realizing these constraints by simply constructing all brane combinations for the rectangular torus, relating m_i in the construction to $2\tilde{m}_i$ and imposing the additional condition that on a tilted torus there must be an even number of any brane with $n_i \not\equiv m_i \pmod 2$, corresponding to half that number of branes with twice the n_i and $\tilde{m}_i$ equal to that m_i. (For several tilted tori, each tilted direction in which $n_i \not\equiv 2\tilde{m}_i$ requires that we double the effective number of branes in the counting for rectangular tori to get a single brane on the tilted tori). Note that when a subset of tori are tilted, the permutation symmetry on tadpoles is broken. In particular, this means that a brane configuration on rectangular tori may give several configurations with 1 or 2 tilted tori, depending on which torus/tori is/are tilted. For example, the single **A**-brane of (3.22) is a valid **A**-brane (using $m_i \to 2\tilde{m}_i$ on the tilted tori) if either the first or second torus is tilted, but not if the third torus is tilted since $n_3 \not\equiv 2\tilde{m}_3 \pmod 2$. If we are counting all **A**-brane combinations with the first torus tilted, then, after using the permutation symmetry (3.22) gives the allowable **A**-branes

$$(-168, 3, 7, 8)_{(3,1\tilde{/}2;7,1;-8;-1)}, \qquad (-168, 7, 3, 8)_{(7,1\tilde{/}2;3,1;-8;-1)} \tag{3.23}$$

where the tilde denotes winding numbers $\tilde{m}_i$ on the tilted torus. We have computed the number of **A**-brane configurations with 1, 2, and 3 tilted tori in this fashion. The results are given in table 3.

4 Models containing gauge group G

Using the set of all possible configurations of **A**-branes, as described in the previous section, it is possible to efficiently generate all brane configurations which realize many features of interest. In particular, given any fixed gauge group G it is possible to construct all distinct brane combinations which realize this gauge group as a subgroup of the full gauge group in any model in polynomial time. In principle, construction of all SUSY models is possible, but this is computationally intensive as the total number of models is quite large.

There are several reasons for focusing on the problem of constructing all realizations of a fixed group G rather than simply enumerating all models. This approach significantly simplifies the computational complexity, while still extracting some of the most interesting

JHEP06(2009)073

data. From a purely model-building perspective, say one is interested in constructing all standard-model like brane configurations. For a given realization of the group $G_{321} = \mathrm{SU}(3) \times \mathrm{SU}(2) \times \mathrm{U}(1)$ in terms of a set of $3 + 2 + 1$ branes, there may be a large number of ways of completing the configuration to saturate the tadpole equations. But much of the physics of the model, such as the number of generations of "quarks" carrying charge under SU(3) and SU(2) depends only on the choice of branes to realize G and is independent of the way in which this model is completed with extra branes. The extra branes may generate a hidden sector or chiral exotics which are of interest, but it is probably more efficient for model building purposes to first consider all realizations of G, and then to explore the possible extra sectors only of those realizations which have physical properties of interest.

From a more general point of view, the purpose of constructing all configurations with fixed gauge subgroup G is to get a clear handle on what the important factors are which control the distribution of models. By considering the variety of ways in which a gauge subgroup like $G = \mathrm{SU}(3) \times \mathrm{SU}(2)$ can be realized in any SUSY IBM model on $T^6/\mathbb{Z}_2 \times \mathbb{Z}_2$, for example, we gain insight into the mechanism responsible for generating the bulk of these configurations. This also provides a clear way to analyze more detailed features of these constructions such as the number of generations of matter fields in various representations.

In the first part of this section (subsection 4.1) we describe the general method of computing all brane configurations which generate a gauge subgroup G; we then explicitly compute all such configurations for gauge groups $\mathrm{U}(N)$ in subsection 4.2 and $\mathrm{SU}(3) \times \mathrm{SU}(2)$ in subsection 4.3. By looking at the distribution of these gauge groups and associated tadpoles, we gain insight into how the diversity of realizations of these groups is associated with **A**-branes with large negative tadpoles, as well as providing useful tools for model building. We also construct all brane configurations realizing $\mathrm{SU}(N) \times \mathrm{SU}(2) \times \mathrm{SU}(2)$ in 4.4. In 4.5 we discuss the K-theory constraints and how they can reduce the total number of allowed realizations of any fixed G. Finally, in subsections 4.6 and 4.7 we relate the results described here to earlier work on IBM model building on this and other toroidal orbifold models.

4.1 Systematic construction of brane realizations of G

As mentioned above, the problem of finding all ways in which a fixed group G can be realized as a subgroup of the full gauge group can be solved in a straightforward way in polynomial time given the results of the section 3. Any complete model containing a set of branes individually satisfying the SUSY constraints for a common set of moduli and collectively solving the tadpole and K-theory constraints, contains either no **A**-branes or some given set of **A**-branes which must be one of the 99,479 configurations enumerated above. Given a configuration of **A**-branes, there is a finite number of ways in which **B**- and **C**-branes can be added to saturate the tadpole conditions, since the **B**- and **C**-branes have only positive tadpoles. Thus, to determine all realizations of G, we just need to run through each of the roughly 10^5 possible **A**-brane combinations and for each determine all realizations of G through adding **B**- and **C**-branes to the given **A**-brane combination without oversaturating the tadpole constraints.

JHEP06(2009)073

To be explicit, say we want to find all models containing the gauge group $G = \mathrm{SU}(N_1) \times \mathrm{SU}(N_2) \times \ldots \times \mathrm{SU}(N_r)$. Each of the r stacks can be made up of **A** , **B** or **C** type branes (for **A**- and **B**-branes $\mathrm{SU}(N_i)$ would be realized as a subgroup of $\mathrm{U}(N_i)$, while for **C**-branes, $\mathrm{SU}(N_i)$ would be realized as a subgroup of a symplectic group $\mathrm{Sp}(N)$ as discussed in more detail below).

The first step in explicitly constructing all realizations of G is looping through our list of all **A**-brane configurations. For each **A**-brane configuration we see if there are N_i duplicates of any brane. If so, then these N_i **A**-branes can provide a factor of $\mathrm{U}(N_i)$ to the gauge group. We form all possible combinations of branes in the **A**-brane configuration which can be used to compose parts of the group G, with the remaining parts arising from extra branes which must be added to the model. For each of these realizations of a subgroup of G by some branes in a configuration of **A**-branes, we then consider all possibilites of **B** and **C** type branes that can be added in stacks to fill out the remaining needed components of G.

Algorithmically, adding **B**-branes to the configuration of **A**-branes is straightforward. Since we have already included all the **A**-branes that will go into the configuration, and since **B**-branes have only positive tadpoles, all the tadpoles will be bounded by the tadpole constraint. Thus, to find all ways of including a stack of **B**-branes which are compatible with a given **A**-brane combination, we proceed by scanning over possible winding numbers of the **B**-brane to be added that are consistent with the tadpole constraints. Once a compatible stack of N **B**-branes is found, we check to see if this **B**-brane along with the branes already in the configuration satisfy the SUSY condition, by confirming that the resulting constraints on moduli are compatible. All possible ways of adding **B**-brane stacks within the tadpole constraints can be constructed in this fashion. The addition of stacks of **C**-branes is even simpler, since there are only four different **C**-branes that can be added and the **C**-branes do not affect the SUSY conditions.

After constructing the set of all realizations in this way, we may have multiple instances of the same realization, for example associated with different extra **A**-brane configurations. To reduce the final set of configurations to a single instance of each equivalent realization, we must drop the extra branes, put each configuration in some canonical form, and drop copies. Note that in this class of brane configurations we have a clear criterion for determining equivalence of solutions, using the symmetries described in section 2.2, unlike for example the situation described in [23].

Thus, in a straightforward way we can scan over all possible inequivalent ways of building the gauge group G from **A**-, **B**-, and **C**-brane stacks in a way which is compatible with the supersymmetry and tadpole constraints. Note that we are not checking the K-theory constraints at this stage, since we are only generating a subset of the complete set of branes in any given model. Thus, the set of realizations generated through this algorithm may be over-complete. While generically additional branes can be added in many ways, some of which will satisfy the K-theory constraints, in some cases, particularly when our realization of G comes close to satisfying the tadpole constraints, there may be no complete model containing this realization which satisfies the K-theory constraints. This must be checked in a case-by-case fashion for models of interest.

JHEP06(2009)073

We have so far concentrated on the case when the tori are untilted. For tilted tori we proceed as discussed above for enumerating **A**-brane stacks. We only keep configurations where there are an even number of branes with $n_i \not\equiv m_i = 2\tilde{m}_i$ on the tilted tori, noting that the resulting gauge group for a stack of $2^k N$ such branes with $n_i \not\equiv m_i$ on k tilted tori is U(N). Practically, we can find configurations realizing a desired gauge group on a compactification with tilted tori by computing the configurations on untilted tori, and then checking whenever there is a stack of N branes with $n_i \not\equiv m_i$ on k tilted tori that an additional $N(2^k - 1)$ branes of this kind can be added without oversaturating the tadpole conditions. (For the **A**-branes, we just need to confirm that there are an additional $N(2^k - 1)$ of these branes available in the **A**-brane combination used at the first step of the analysis.) Clearly, this means that with more tilted tori there will be fewer realizations of G.

4.2 Realizations of SU(N)

As a simple example, we consider the construction of all possible brane realizations of the group SU(N) as a subgroup of the full gauge group. There are 3 ways in which the group SU(N) can be realized.

(i) The group SU(N) can be realized as a subgroup of the U(N) associated with N identical **A**-branes[5]. To identify all ways in which this can be done we just need to scan over all 10^5 known **A**-brane combinations for configurations including N copies of the same brane, and then list all **A**-branes for which N copies appear in some **A**-brane combination.

(ii) The group SU(N) can be realized, again as a subgroup of U(N), through N identical **B**-branes. For each combination α of **A**-branes, we look at all possible ways in which a **B**-brane β can be chosen so that combining N copies of β with α gives total tadpoles which are all $\leq T$. This condition puts strong constraints on the winding numbers of β. For each β which combines with α without exceeding the tadpole constraints, a further check must be done that the system of linear equations given by the SUSY equalities (2.6) for the branes in α and β admit at least one solution. Finally, symmetries must be considered so that only one example of each such β configuration is included in a final list. (While the same brane stack β may be associated with many different **A**-brane combinations α, these represent "extra" branes in the same way as additional **B**-branes or **C**-branes completing the tadpole constraints, so do not really realize distinct realizations of SU(N).)

(iii) The group SU(N) can also be realized as a subgroup of Sp(N) arising from N identical **C**-branes. Checking for this possibility for each combination α of **A**-branes is straightforward; any total tadpole of α which is less than $T - N$ can be associated with N additional **C**-branes. The value $N = 2$ is a special case, since SU(2) = Sp(1),

[5]Note that when SU(N) is realized as a subgroup of U(N), as in *i*) and *ii*), the extra U(1) factor often becomes anomalous and gets a mass through the Green-Schwarz mechanism [24, 25].

JHEP06(2009)073

type\N	U(1)	2	3	4	5	6	7	8	> 8	> 520
A	3259	250	59	17	8	3	1	1	0	0
B	7067	1144	377	151	82	39	15	1	0	0
C	1	1	1	1	1	1	1	1	1	0

Table 4. Numbers of distinct ways in which SU(N) (U(1) for $N = 1$) can be realized by **A**, **B**, or **C**-type branes as a subgroup of the full gauge group (with untilted tori).

so SU(2) can be realized from a single **C**-brane. Since there is really, up to symmetry, only one possible stack of N **C**-branes, there is one possible realization of each SU(N) as a subgroup of Sp(N) up to the maximum of $N = 520$, which can be realized in the presence of the **A**-brane (3.20). There is one more subtlety here relevant for model-building. Although the group SU(N) can be realized as a subgroup of Sp(N) with N **C**-branes, the fields transforming only under that Sp(N) live in the antisymmetric representation and cannot break Sp(N) down to only SU(N). By turning on bifundamentals, for example between two stacks of N **C**-branes with different tadpoles, the symmetry can be broken down to SU(N); this corresponds to brane recombination, giving a different set of branes. Alternatively, if we have $2N$ **C**-branes, these branes can be moved away from the orientifold plane, giving a gauge group U(N) $\supset$ SU(N), as described in [16]. Using this mechanism, the largest SU(N) which can be realized without the remainder of an Sp(N) is SU(260) by 520 **C**-branes in combination with (3.20).

We have carried out the necessary computation for each type of brane. The number of distinct realizations of SU(N) in terms of **A**-branes, **B**-branes, and **C**-branes is shown in table 4.

Most of the realizations of SU(N) arise from stacks of N **B**-branes. To understand the origin of the numbers in this table more clearly let us consider the case of SU(7) $\subset$ U(7) arising from 7 identical **B**-branes. Each **B**-brane has two nonvanishing tadpoles, so up to symmetries the **B**-brane involved has tadpoles $(P, Q, 0, 0)$ with $P \geq Q > 0$, so the full U(N) stack has total tadpole $(7P, 7Q, 0, 0)$. Since every **A**-brane combination has at most one negative tadpole, we must have $Q = 1$. This constrains the winding numbers n_1, m_2, m_3 to be unity (with canonically chosen signs), so that the only freedom is in winding numbers n_2, n_3 with $P = n_2 n_3$. In the absence of any **A**-branes, we can only have $P = 1$. Any **A**-brane combination included must have total $Q = 1$, and $P < 0$. Among single **A**-branes, the one with the most negative tadpole and $Q = 1$ is

$$\alpha_{64} = (-64, 1, 8, 8)_{(1,1;8,1;-8,-1)} \,. \tag{4.1}$$

With more **A**-branes, constrained to have total $Q = 1$, the negative tadpole decreases rapidly in absolute value. For two **A**-branes, for example, the most negative P tadpole comes in the combination $(-9, 1, 7, 8) = (-24, 2, 3, 4)_{(2,1;3,1;-4,-1)} + (15, -1, 5, 3)_{(1,-1;5,1;3,1)}$. A single **A**-brane and a single **B**-brane of this type are always compatible under SUSY.

JHEP06(2009)073

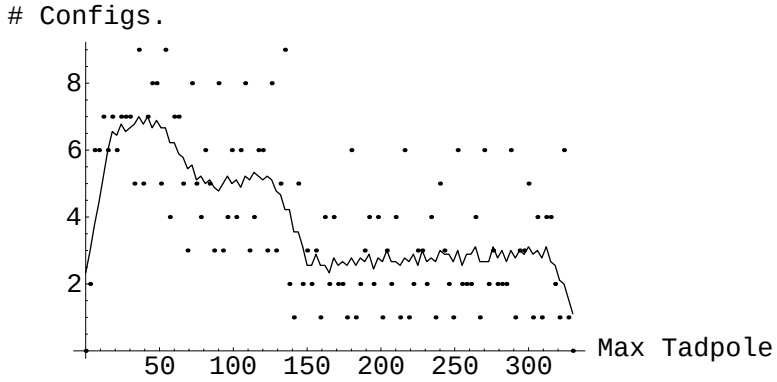

Figure 2. Distribution of the maximum tadpole for the 3 branes forming each of the 437 distinct SU(3) realizations. Solid curve is data averaged over window including the nearest 4 data points in each direction for clarity (untilted tori).

Thus, the set of possible **B**-branes giving U(7) is just the set of n_2, n_3 with $7n_2n_3 \leq 72$, where we can choose $n_2 \geq n_3$ using the permutation symmetry between the second and third tori. There is no relative primality constraint as these winding numbers are on different tori. There are precisely 15 such combinations, giving the entry in the table above.

A similar story holds for U(N) with smaller N arising from a stack of N identical **B**-branes. For $N = 6$, the **A**-brane can have $Q = 2$, which allows $P = -128$. The number of $n_2 \geq n_3$ with $6n_2n_3 \leq 136$ is 39, as in table 4. The story is slightly more complicated for $N \leq 4$, since then the **B**-brane can have $Q > 1$, but a similar analysis shows that precisely the number of **B**-branes indicated in table 4 can be included N times in a model, almost always with a single additional **A**-brane.

This analysis gives the first clear example of one of the primary conclusions of this paper: the greatest diversity of configurations realizing a particular feature (such as a fixed subgroup of the full gauge group) arises in association with one or sometimes more "extra" **A**-branes. These **A**-branes lie in the tail of the distribution and give a very negative tadpole allowing "phase space" for the range of winding numbers. Indeed, most of the **B**-brane stacks giving rise to the range of SU(N) configurations have a single large positive tadpole, requiring a single extra **A**-brane with a very negative tadpole. A simple way to see this is to graph the distribution of the largest positive tadpole associated with the stack of N branes giving the SU(N) gauge group. The distribution of maximum total tadpoles for the 3 branes giving the SU(3) in the case $N = 3$ is graphed in figure 2. For these configurations the maximum tadpole ranges from 3 through 327 (this number includes the factor of 3 from the stack of 3 branes). Most of these tadpoles are quite large compared to the negative tadpole of a typical **A**-brane combination. Indeed, over 75% of the SU(3) realizations have a maximum tadpole contribution above 50, and can only be realized with single **A**-branes in the tail of the distribution shown in figure 1. The distribution in figure 2 is rather discontinuous due to the small numbers of configurations involved.

JHEP06(2009)073

A statistical analysis of models containing the group SU(5) was carried out in [26]. They found almost 7000 models containing the group SU(5) at small moduli. This number is much greater than the number 91 in table 4 giving the number of distinct realizations of SU(5) since they include all possible configurations of additional branes saturating the tadpole condition to form complete models. In fact, most of the 7000 models they produced most likely come from a small subset of the 91 distinct SU(5) configurations, since those with large winding numbers produce larger moduli. We discuss related issues in more detail in section 5.

4.3 Realizations of $\mathrm{SU}(3) \times \mathrm{SU}(2)$

As a somewhat more complex example we have computed all realizations of $G = \mathrm{SU}(3) \times \mathrm{SU}(2)$. As described in subsection 4.1 we can systematically find all such realizations by first considering all **A**-brane combinations, finding all ways one or both components of the gauge group can be included in the **A**-brane combination, and then adding stacks of **B**- or **C**-branes to complete the group G, including cases where both the SU(3) and the SU(2) come from **B**- or **C**-branes. This group is of obvious phenomenological interest, as every standard-model like construction in this framework must contain at a minimum the group $G = \mathrm{SU}(3) \times \mathrm{SU}(2)$ as a subgroup. So finding all possible constructions of this group represents a step towards identifying all realizations of standard-model like physics in any class of compactifications.

4.3.1 Enumeration of distinct realizations for $\mathrm{SU}(3) \times \mathrm{SU}(2)$

There are 9 different ways in which the different types of branes can be combined to form the group G. The numbers of ways in which this can be done (without tilted tori) are tabulated in table 5. Note that we are only requiring a single **C**-brane for $\mathrm{SU}(2) = \mathrm{Sp}(1)$, and including configurations with 3 **C**-branes where $\mathrm{SU}(3) \subset \mathrm{Sp}(3)$, although as discussed in 4.2 additional branes are needed to allow the breaking of $\mathrm{Sp}(N)$ to just SU(3). (Configurations where 6 **C**-branes realize SU(3), so that the reduction $\mathrm{Sp}(6) \to \mathrm{SU}(3)$ is possible by brane splitting, are indicated in parentheses.) Thus, we are solving the mathematical problem of finding all realizations of $\mathrm{SU}(3) \times \mathrm{SU}(2)$ in any way that it can be realized as a subgroup of the full gauge group (including when the branes are the same, giving a group SU(5)). This includes any possible configuration which would lead to a model containing any extension of the standard model, but not every configuration constructed here will correspond to a full model with explicit $\mathrm{SU}(3) \times \mathrm{SU}(2)$ gauge subgroup. Each of the configurations found here can be extended in one or more ways to a full model, for which the K-theory constraints must be checked.

Of the total of 171,655 constructions of G, by far the greatest number arise from combinations of **B**-brane stacks. Again, in most cases there is a single extra **A**-brane needed to push down the total tadpole. In the presence of this **A**-brane there is a tradeoff between **B**-branes and **C**-branes in the "phase space" of brane configurations. When T is large there are many more **B**-branes than **C**-branes possible within the tadpole limits, while when T is small, **C**-branes contribute smaller tadpoles and are easier to add. In this situation, while $T = 8$ is reasonably small, the wider range of possibilities for **B**-branes

JHEP06(2009)073

3 \ 2	**A**	**B**	**C**
A	84	939	169
B	1802	164057	1274
C	554 (316)	2774 (1595)	2 (2)

Table 5. Numbers of distinct ways in which $G = \mathrm{SU}(3) \times \mathrm{SU}(2)$ can be realized through combinations of **A**-, **B**-, and **C**-branes (untilted tori). Numbers in parentheses are for $\mathrm{SU}(3) \subset \mathrm{Sp}(6)$.

wins out and these provide the widest range of possible realizations of the desired gauge group. Of the more than 164,000 combinations of 3 **B**-branes with one set of winding numbers and 2 **B**-branes with another set of winding numbers, all but 2 configurations can be realized with either no **A**-branes or a single **A**-brane. These two exceptional cases are given by

$$3 \times (0,4,1,0)_{(2,1;1,2;0,-1)} + 2 \times (0,0,1,2)_{(0,-1;1,2;1,1)}$$
$$3 \times (2,0,1,0)_{(2,1;1,0;1,-1)} + 2 \times (0,0,1,8)_{(0,-1;1,8,1,1)}$$

Each of these two cases requires two additional identical **A**-branes, $2 \times (4,-2,1,2)_{(2,-1;1,1;2,1)}$ in the first case, and $2 \times (1,4,1,-4)_{(1,1;1,4;1,-1)}$ in the second. The integer moduli are uniquely fixed in both cases, to $(h,j,k,l) = (8,1,4,4)$ and $(h,j,k,l) = (8,1,16,1)$ respectively.

As in the $\mathrm{SU}(N)$ case discussed in the previous subsection, it is helpful to graph the distribution of maximum total tadpole to get a sense of the distribution of models. In figure 3 we graph the number of realizations of $\mathrm{SU}(3) \times \mathrm{SU}(2)$ with different maximum total tadpole contributions (including only configurations composed of **B**- and **C**-branes). As in the SU(3) case, most of these tadpoles are only compatible with a single extra **A**-brane with a very negative tadpole in the tail of the distribution. As discussed above, the sets of realizations computed here are overcomplete, since many of these configurations cannot be completed to complete models compatible with the K-theory constraints. We describe this reduction in more detail in subsection 4.5.

While the focus of this paper is not on realistic model building, and is rather on developing general methods and a systematic understanding of the space of models on the $T^6/\mathbb{Z}_2 \times \mathbb{Z}_2$ orientifold, it is interesting to push this construction slightly further in the model-building direction to get further information about the distribution of models in this framework. To this end, we have considered increasing the gauge group to $\mathrm{SU}(3) \times \mathrm{SU}(2) \times \mathrm{U}(1)$; we have also studied the distribution of "quark" generation numbers in the complete set of $\mathrm{SU}(3) \times \mathrm{SU}(2)$ realizations just described. We briefly describe these further studies in the remainder of this subsection.

4.3.2 Gauge group $\mathrm{SU}(3) \times \mathrm{SU}(2) \times \mathrm{U}(1)$

We have generated all realizations of the larger gauge group $G_{321} = \mathrm{SU}(3) \times \mathrm{SU}(2) \times \mathrm{U}(1)$, where the $\mathrm{SU}(3) \times \mathrm{SU}(2)$ brane configurations described above are extended with one more brane of either **A**, **B**, or **C**-type (i.e., the U(1) does not come solely from U(3) and/or

JHEP06(2009)073

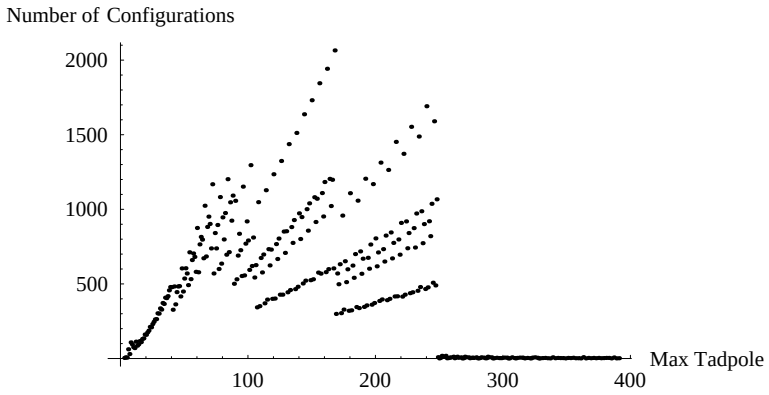

Figure 3. Number of distinct SU(3) × SU(2) configurations of **B**/**C**-branes (on untilted tori) with given maximum total tadpole. Form of distribution shows most configurations are only possible with addition of an extra **A**-brane with a large negative tadpole.

U(2) groups in which the SU(3), SU(2) are embedded). For the case when none of the tori are tilted, there are approximately 13.7 million distinct ways of realizing this larger gauge group. About half of these configurations come from having a 3-stack of **C**-branes with a 2-stack of **B**-branes and a 1-stack of **B**-branes, along with 1 extra **A**-brane (we can write this as 3C × 2B × 1B with extra A). The majority of the other half of the configurations come from an extra A-brane with 3B × 1C × 1B (with SU(2) = Sp(2)) or 3B × 2B × 1B, or 3B × 2B × 1A. As discussed above, the balance between **C**-branes and **B**-branes in the construction depends on the tadpole T, which in this case is at an intermediate point where the smaller contribution of **C**-branes competes well with the larger number of possible **B**-branes in forming the SU(3) part of the group. As in the case of SU(3) × SU(2), we graph the maximum total tadpole from each brane configuration forming SU(3) × SU(2) × U(1). The number of configurations with a given maximum total tadpole peaks around a tadpole of 100, indicating that almost all of these configurations depend upon an extra **A**-brane with a highly negative tadpole. Note that the large number of configurations involved gives the graph in figure 4 a much smoother appearance than the corresponding graphs for SU(3) or SU(3) × SU(2) depicted in figures 2, 3, although the discrete nature of the constraint problem becomes apparent at larger values of the tadpole. As above, the configurations graphed in figure 4 do not represent complete models.

4.3.3 Tilted tori

We have carried out the computation of the number of distinct brane combinations satisfying SUSY and tadpole constraints and realizing groups SU(3) × SU(2) and SU(3) × SU(2) × U(1) (again, with an independent U(1)) for any number of tilted tori from 0 through 3. The number of configurations for the four cases is given in table 6.

As the number of tilted tori is increased, the number of models decreases substantially. As discussed previously, this makes sense since we can effectively treat models on tilted

JHEP06(2009)073

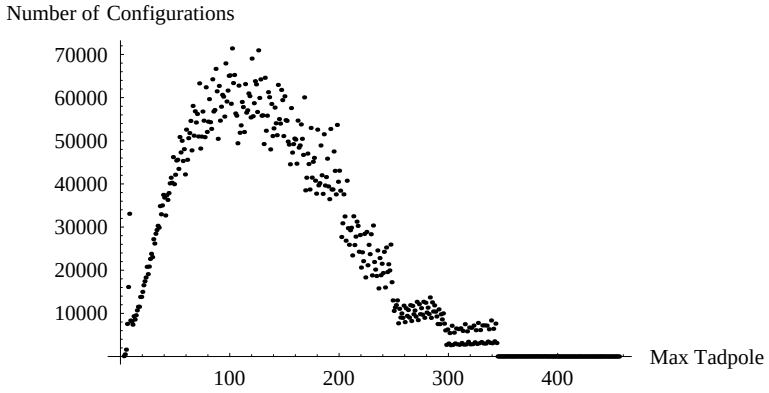

Figure 4. Number of distinct SU(3) × SU(2) × U(1) brane configurations (on untilted tori) with given maximum total tadpole. Form of distribution with peak around 100 shows most configurations are only possible with addition of an extra **A**-brane with a large negative tadpole.

Number Tilted Tori	0	1	2	3
Number 3-2 Configurations	171,655	44,658	2,026	40
Number 3-2-1 Configurations	13,724,917	2,406,352	103,652	1,222

Table 6. Number of 3-2 and 3-2-1 configurations.

tori as a subset of models on rectangular tori, where branes with opposite parity winding numbers on tilted tori must appear even numbers of times.

The dramatic increase in the number of possible configurations when an extra U(1) brane is included illustrates the rapid combinatorial growth of the total number of models when additional branes are included. Indeed, typical 3-2-1 configurations are compatible with $\mathcal{O}(10)$ distinct combinations of extra **A**-branes. In the enumeration of such configurations, which began with distinct **A**-brane configurations and added branes in all ways to realize G_{321}, before we deleted duplicate configurations to obtain the 13.7 million distinct 3-2-1 configurations, there were $\mathcal{O}(10^8)$ configurations including **A**-brane information.

For any specific realization of $G = \mathrm{SU}(3) \times \mathrm{SU}(2)$, all possible combinations of extra branes which saturate the tadpole condition could be determined. In principle this could be done for all models, but it would lead to hundreds of millions, probably billions of total models, so a fairly extensive computer project would be involved. Since much of the relevant physics (such as the matter content in the bifundamental representations of the group G) can be determined just from the construction of G, it seems more pragmatic to approach any systematic attempt to model building by first constructing the gauge group of interest, and then isolating the subset of models with further desired properties. After this, the set of extra branes giving rise to additional gauge groups and hidden or exotic matter can be systematically determined.

JHEP06(2009)073

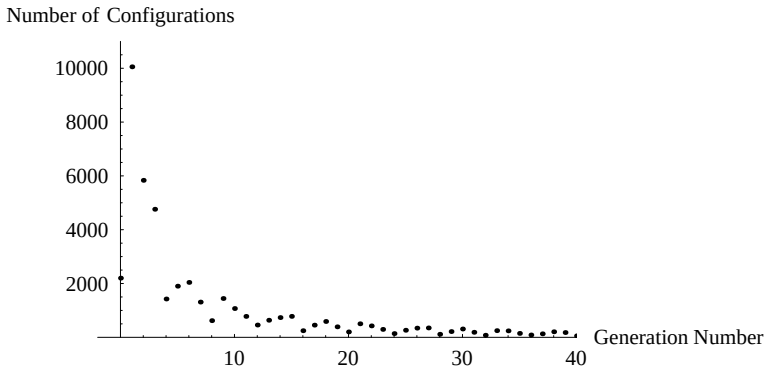

Figure 5. Distribution of number of "quark" generations for SU(3) × SU(2) configurations with a single tilted torus.

4.3.4 Distribution of generation numbers

In [20, 21], a variety of models were considered and correlations between gauge group and generation numbers were studied. In general, it was found that there was no strong correlation between gauge group and generation numbers. We have explicitly computed the numbers of generations of "quarks" which transform in the fundamental representation of SU(3) and the antifundamental (which is equivalent to the fundamental) representation of SU(2), for the various brane configurations tabulated in table 5. As discussed in section 2.2, only when there is at least one tilted torus can there be an odd intersection number between branes which are not **C**-branes.

We have analyzed the intersection numbers of all the configurations described above giving SU(3) × SU(2) in the case of one tilted torus. The sum of intersection numbers $I_{32} + I_{32'}$, which gives the number of "quark" generations, is computed for all 44,658 of these configurations (using only I_{32} when the SU(2) comes from a **C**-brane), and the resulting distribution is graphed in figure 5.

The number is peaked at 1, and drops off fairly rapidly, with typical generation numbers of order $\mathcal{O}(10)$. There is no particular enhancement or suppression of 3 generations; 4760, or about 10% of the configurations have 3 generations of "quarks". Thus, 3 generations seems roughly typical of these models (though note that the 170 thousand configurations with no tilts have even numbers of generations except in a few cases with **C**-branes, so in the total set of configurations odd generations are less frequent).

Almost all (4704) of the 3-generation configurations have SU(3) × SU(2) realized by 3 **B**-branes of one kind and 2 **B**-branes of another kind. An example of one of the 3**B**× 2**B** configurations realizing SU(3) × SU(2) with 3 generations of matter in the bifundamental of the gauge groups is

$$3 \times (0,9,1,0)_{(3,\widetilde{1/2};1,3;0,-1)} + 2 \times (0,13,0,1)_{(1,\widetilde{1/2};0,-1;1,13)} \tag{4.2}$$

This combination of branes requires at least one **A**-brane to bring the tadpoles down. Over

JHEP06(2009)073

a dozen individual **A**-branes can be combined with (4.2) to reduce all the tadpoles to below the bound. One example of such an **A**-brane is

$$(6, -45, 5, 6)_{(3,\widetilde{1/2};1,-3;2,-5)} \tag{4.3}$$

Just including this **A**-brane with the branes (4.2) and including 2 **C**-branes with nonzero tadpoles P as fillers gives a model with total gauge group (before removing anomalous U(1) factors) $\mathrm{U}(3) \times \mathrm{U}(2) \times \mathrm{U}(1) \times Sp(2)$. Solving the SUSY equations (that is, solving (2.6) for integer moduli with the branes (4.2), (4.3) using $\tilde{m}_1$ in place of m_1) shows that the moduli for this model are $h = 4, j = 279, k = 26, l = 2$ (well outside the range studied in [20]). Typical of such constructions, this model has additional exotic massless chiral matter fields charged under the $\mathrm{SU}(3)\times\mathrm{SU}(2)$ part of the gauge group, coming from nonzero intersections between the branes (4.2) and the other branes in the model. So this is not a realistic model of nature, but provides an example of one of the many ways that branes can consistently combine to form models with gauge group containing $\mathrm{SU}(3) \times \mathrm{SU}(2)$ as a subgroup with 3 generations of "quarks". All of the 4760 configurations with 3 generations are compatible with at least one **A**-brane configuration (and generally many) in such a way as to satisfy the tadpole and SUSY constraints. One might also worry about K-theory constraints for complete models, but these may be weaker when at least one torus is tilted [27]. We will not say more here about these 4760 realizations of $\mathrm{SU}(3) \times \mathrm{SU}(2)$ with 3 generations of quarks, leaving this to further work. Clearly, however, these models form a good starting point for a systematic analysis of models with features of the standard model.

We have focused here on the case of a single tilted torus, where generally the SU(3) and SU(2) components of the gauge group are both realized by **B**-branes. It is also worth considering the situation where the SU(2) comes from a **C**-brane on the orientifold plane with Sp(1) gauge group. In this case, the intersection number I_{32} between the branes forming the SU(3) and the **C**-brane can be odd even with no tilted tori. We have found that this intersection number is 3 in 49 distinct cases. Of these 49, 4 have the SU(3) realized by an **A**-brane (in each case having a tadpole > 8 requiring another **A**-brane to fix tadpoles), and 45 have the SU(3) realized by a **B**-brane. One of the simplest examples, where the **B**-brane is $(0, 1, 9, 0)_{(1,3;3,1;0,-1)}$ and the **C**-brane is $(0, 0, 0, 1)_{(0,1;0,-1;1,0)}$ was used in [15–17] to construct a semi-realistic 3-generation model. Most of the other examples have much larger tadpoles, such as realizing the SU(3) by $3 \times (0, 2, 39, 0)_{(1,13;3,2;0,-1)}$, which obviously requires an additional **A**-brane with large negative R tadpole.

A more complete analysis would be needed to determine which of the realizations considered in this subsection can be completed to models with additional branes saturating the tadpole conditions and the K-theory constraints. One could in principle look for further structure reminiscent of the standard model in a straightforward fashion by including the U(1) and possibly extending the gauge group further and computing the resulting possibilities for further matter content. We leave this endeavor to further work.

4.4 Realizations of $\mathrm{SU}(N) \times \mathrm{SU}(2) \times \mathrm{SU}(2)$

As a further application of the method, we have constructed all realizations of the gauge group $\mathrm{SU}(N) \times \mathrm{SU}(2) \times \mathrm{SU}(2)$ for various values of N. This gives a picture of how adding

JHEP06(2009)073

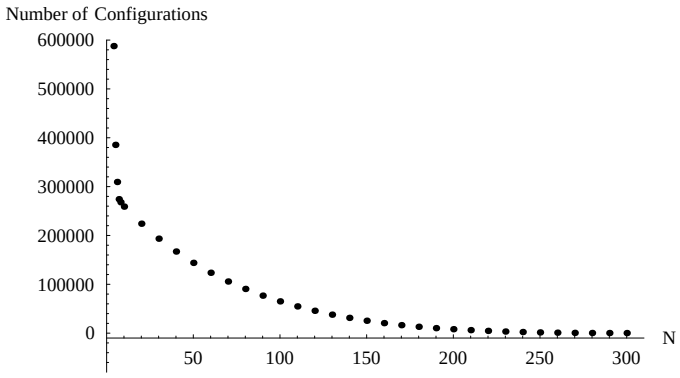

Figure 6. Number of distinct brane configurations giving SU(N) × SU(2) × SU(2) (untilted tori).

additional components to the gauge group increases the number of constructions including SU(N). Also, the case $N = 4$ is relevant to construction of semi-realistic Pati-Salam models as discussed in subsection 4.6 .

The number of realizations of this group for various values of N is plotted in figure 6. For example, the number of distinct realizations of SU(4) × SU(2) × SU(2) is 587,704. Starting with $N = 4$, the majority of solutions are of the form $NC \times 2B \times 2B$ with a hidden **A**-brane, for reasons similar to those discussed above for the SU(3) × SU(2) × U(1) models. Starting from $N = 8$, the U(N) brane has to be a **C**-brane (since a stack of 8 or more **B**-branes would oversaturate two of the tadpoles, and one or more extra **A**-branes can only compensate for one of the excess tadpoles). There is thus a steady reduction in the number of configurations as N increases. The hidden **A**-brane with the most negative possible tadpole is of the form $(P, Q, R, S) = (-512, 8, 8, 8)$. Thus at $N = 518$, there is only one realization, in which the group SU(518) × SU(2) × SU(2) arises as a subgroup of Sp(520) composed of 520 identical **C**-branes with tadpoles $(1, 0, 0, 0)$. There are no brane constructions compatible with tadpole constraints for $N > 518$.

4.5 K-theory constraints

Because we have focused here on constructing distinct brane configurations of a given G as a subgroup of the full gauge group, and not on the details of how such configurations can be expanded to complete models saturating the tadpole constraints, the K-theory constraints do not apply directly to the configurations we have constructed. To test the K-theory constraints for a given configuration, we must first add additional **B**- and **C**-branes to the configuration to give a complete model which saturates the tadpoles, and then test K-theory for this complete model. For any given configuration there may be many completions to a full model, and consequently many opportunities for satisfying the K-theory constraints. We find, however, that for some configurations there are no completions at all to models satisfying the full K-theory constraints. Additionally, these constraints have a stronger impact on the range of allowed configurations further out in the tail of the distribution where the dominant set of configurations arises from a single **A**-brane with a very negative tadpole. This enhanced K-theory suppression of the tail arises in part from the smaller

JHEP06(2009)073

number of completions possible from a given realization of G to a complete model saturating the tadpoles, and in part from discrete effects associated with the integer constraints on the problem.[6]

To get a sense of how the K-theory constraints affect the distribution of models containing a particular realization of G, we have considered the set of SU(3) $\times$ SU(2) brane realizations through a combination of a stack of 3 **B**-branes and a stack of 2 **B**-branes, with an arbitrary **A**-brane combination included to provide "phase space". As discussed above, there are some 164,000 distinct 3**B** $\times$ 2**B** configurations which can be realized in this way in a fashion consistent with supersymmetry and the tadpole constraints. While in general there are multiple ways in which each such realization can be expanded to a complete model (before checking K-theory) by saturating the tadpole constraints, one such way of building a complete model is simply including "filler" **C**-type branes to saturate the tadpole. Such **C**-branes do not affect the K-theory conditions. We have checked the K-theory constraints for the **C**-brane completions of this set of models. We find that in fact the K-theory conditions substantially constrain the range of valid constructions. While the distribution still has a long tail, only 3636 of the 164,000 **C**-brane completions of the 3**B** $\times$ 2**B** combinations are compatible with the K-theory constraints. Furthermore, the K-theory constraint suppresses configurations with larger tadpoles more strongly. Of the allowed configurations, the average of the maximum total positive tadpole for the **B**-branes is around 32, and the maximum of this quantity is 68, much smaller than for the distribution without K-theory constraints shown in figure 3. It is interesting to note that K-theory reduces the number of models possible with a single **A**-brane. Whereas before the K-theory constraints are imposed all but 2 of the 164,000 **B**-brane 3-2 combinations can be constructed with a single extra **A**-brane, when K-theory is imposed on the **C**-brane completions of the configurations, only 3457 of the 3636 distinct models are compatible with a single **A**-brane. Including other possible completions by **B**-brane combinations to saturate the tadpole may increase the number of allowed configurations substantially. So the number of distinct ways in which SU(3) $\times$ SU(2) can be realized by **B**-branes which can be completed through other branes to a full model satisfying SUSY, tadpole, and K-theory constraints lies somewhere between the lower bound of 3636 (where only extra **A**-branes and **C**-branes are added to give a model satisfying K-theory constraints) and the upper bound of 164,057 (where arbitrary branes can be added and K-theory constraints are not checked). Nonetheless, this analysis suggests that, while the greatest diversity of models is still in the tail of the distribution when K-theory constraints are included, this tail may be truncated substantially by the discrete K-theory constraints when considering complete models of brane combinations saturating the tadpole constraints.

The reason that the K-theory constraints substantially suppress configurations containing a single **A**-brane with a large negative tadpole can be seen from the form of the winding numbers of such branes. All **A**-branes with no tadpoles $Q, R, S > 8$, and one negative tadpole $P < -112$ have the form (with a canonical choice of signs)

$$(P, Q, R, S)_{(n_1,m_1;n_2,m_2;n_3,m_3)} = (-abc, a, b, c)_{(a,1;b,1;-c,-1)} \,. \tag{4.4}$$

[6]Thanks to Robert Richter for suggesting to us the possible role of integer effects in increasing K-theory suppression in the tail, and for helpful discussions on this question.

Such branes contribute a 1 to the first K-theory constraint in (2.9), from $m_1 m_2 m_3 \equiv 1 \pmod 2$. A **B**-brane can only contribute to this K-theory constraint if it has all $m_i \neq 0$, so it has $P = 0$. Such branes reduce the available "phase space" in winding numbers without contributing many possibilities. In particular, forming an SU(3) × SU(2) from **B**-branes where the 3 branes must all have $P = 0$ (necessary to fix the first K-theory constraint in the absence of other **B**-branes) requires that the **A**-brane have Q, R, S tadpoles adding to at most 16 (we need 3×2 for the SU(3), and another 2 for the SU(2)). The most negative tadpole P at which this occurs is for the brane of the form (4.4) with tadpoles (-150, 5, 5, 6), and here supersymmetry rules out the **B**-brane with tadpoles (0, 1, 1, 0). All single **A**-branes with $P < -112$ in combination with $3\mathbf{B} \times 2\mathbf{B}$ and no further **B**-branes are similarly ruled out, so we immediately see that without at least one additional **B**-brane, none of the **B**-brane combinations with maximum total tadpole above 120 contributing to figure 3 can satisfy K-theory. We defer a systematic treatment of all models satisfying the K-theory constraints to further work. We note, however, that the brief discussion here demonstrates that the K-theory constraints significantly decrease the number of configurations associated with large tadpoles, although even the lower bound given here for configurations satisfying K-theory still represents a substantial range of models at moderate tadpoles of order $30-50$. We discuss further aspects of the reduction of the range of allowed constructions in section 5.

4.6 Comparison with previous results on IBM model-building

Many authors have constructed models with various features of the standard model within the framework in which we are working of intersecting branes on the $T^6/\mathbb{Z}_2 \times \mathbb{Z}_2$ orientifold. While the emphasis of this paper is on developing general tools which can be useful either for model-building or for understanding the distribution of models in this corner of the landscape, it is useful to make contact with more detailed model-building results by checking that the specific models found in earlier work are contained within the larger classes of configurations constructed here. We have checked that various supersymmetric standard-model-like constructions in the literature which include SU(3)×SU(2) realizations with 3 generations of quarks are contained within our list of 4760 such configurations. For example, in [13, 14], Cvetič, Shiu and Uranga identified a model containing SU(3) × SU(2) and 3 generations of quarks on the orientifold with one tilted torus using the configuration of **B**-branes (in our notation, with the contribution of $\tilde{m}_1$ to the tadpole doubled)

$$3 \times (1,0,1,0)_{(1,1\tilde{/}2;1,0;1,-1)} + 2 \times (1,0,0,3)_{(1,3\tilde{/}2;1,-1;1,0)} \tag{4.5}$$

as well as additional branes completing the tadpole condition and giving a "semi-realistic" spectrum including an additional gauge sector and exotic chiral matter fields. The intersection numbers between these branes give $I_{32} = 1, I_{32'} = 2$ for a total of 3 generations of "quarks". We have checked that this **B**-brane configuration is in our list of 4760 such configurations. The authors of [13, 14] restricted attention to brane configurations composed completely of **B**-branes, without any extra **A**-branes in the configuration. As discussed above, this severely restricts the range of possible models. Precisely 10 of the 4760 realizations we found of SU(3) × SU(2) with 3 generations of quarks can be constructed without

JHEP06(2009)073

A-branes somewhere in the configuration. Note that the model found in [13, 14] has additional standard-model like features which may not be realizable by adding branes to all the 4760 SU(3) × SU(2) brane configurations with 3 quark generations. We leave a more detailed phenomenological analysis of the range of complete models in which these 4760 brane configurations can be embedded to further work.

Another popular approach to constructing semi-realistic IBM models involves finding a brane configuration giving a Pati-Salam $SU(4) \times SU(2)_L \times SU(2)_R$ group as part of the gauge group, with various additional branes completing the tadpole conditions, and giving additional gauge fields and exotic or hidden matter fields. In [15], a model with 3 generations of matter fields charged under the SU(4) and each of the SU(2)'s was constructed using the **B**-**C**-**C** brane combination

$$4 \times (9,1,0,0)_{(1,0;3,1;3,-1)} + 1 \times (0,0,1,0) + 1 \times (0,0,0,1)\,. \tag{4.6}$$

We have confirmed that this configuration appears in our list of over 5×10^5 realizations of $SU(4) \times SU(2) \times SU(2)$. As pointed out in [17], this brane configuration can be realized in a way compatible with SUSY and K-theory constraints in the presence of the "extra" **A**-branes

$$(-24,2,3,4)_{(-2,-1;3,1;4,1)} + (-24,2,4,3)_{(-2,-1;4,1;3,1)}\,. \tag{4.7}$$

(The addition of **A**-branes to this model to fix the tadpoles was also discussed in [16].)

The use of **C**-branes in (4.6) makes possible the construction of a 3-generation model without tilted tori. This can be realized in other ways; for example in [21] a Pati-Salam model of this type was found where the SU(4) comes from the **A**-brane

$$4 \times (-3,3,1,1)_{(3,1;1,1;-1,-1)} + 1 \times (0,0,1,0) + 1 \times (0,0,0,1) \tag{4.8}$$

where the extra **A**-brane $(6,-4,2,3)_{(2,1;1,-1;3,-2)}$ fixes the tadpole excess, and further **B**- and **C**-branes can be added to saturate the tadpole conditions while containing SUSY and satisfying the K-theory constraints. The 4-2-2 configuration in (4.8) also appears in our complete list of such constructions.

The Pati-Salam models just described use **C**-branes and rectangular tori to realize the SU(2) parts of the model. In [18], Cvetič Li and Liu performed a systematic search for Pati-Salam models where the full $SU(4) \times SU(2) \times SU(2)$ gauge group arises from U(N)'s on stacks of **A**- and **B**-branes, again with 3 generations of matter in the $(\mathbf{4},\mathbf{2},\mathbf{1})$ and $(\bar{\mathbf{4}},\mathbf{1},\mathbf{2})$ representations of the gauge group. This was the first systematic search of this type which included the possibilities of **A**-branes and tilted tori. They found 11 models with the desired properties, including additional constraints on the extra branes needed to saturate the tadpole condition which assist with moduli stabilization and SUSY breaking. We have checked that the brane configurations giving $SU(4) \times SU(2) \times SU(2)$ in all 11 of these models appear in our comprehensive list.

While a number of these "semi-realistic" intersecting brane model constructions which have been analyzed in the literature share many features of the observed standard model of particle physics, all models constructed in this fashion so far also have some unrealistic physical properties. These models generally have exotic massless chiral fermions charged

JHEP06(2009)073

under the standard model gauge group, associated with non-vanishing intersection numbers between the branes forming the standard model gauge group and extra branes which complete the tadpole conditions. Furthermore, while some progress has been made towards incorporating fluxes to stabilize moduli (see for example [17, 29–31]), the intersecting brane constructions have unstabilized moduli appearing as massless scalar fields. A more complete phenomenological model would need to reproduce the standard model spectrum more precisely, as well as stabilize moduli and give a complete picture of supersymmetry breaking (a review of recent developments in using nonperturbative instanton effects to resolve these issues is given in [11]). We also know that the ingredients used in the type IIA orientifold intersecting brane models cannot in principle give a realistic cosmological scenario with many e-foldings of inflation, at least in the supergravity approximation without additional features like NS5-branes [32]. Thus, the models constructed in this fashion should be viewed at this point as prototypes of string constructions of observable physics, which have some desired features and may display interesting characteristics common to more precisely tuned models. The methods we have developed in this paper can be used to isolate sets of IBM models which have particular physical features, which may be useful in further model-building studies. These methods should also be applicable in a wider range of compactifications, such as magnetized brane constructions on a smooth Calabi-Yau where a much larger range of constructions should be possible, and therefore more detailed features of observed physics should be realizable.

4.7 Other toroidal orbifolds

In this paper we are focused on the $T^6/\mathbb{Z}_2 \times \mathbb{Z}_2$ orientifold. A number of other toroidal orbifolds have been considered in the literature [1]. The $T^6/\mathbb{Z}_2 \times \mathbb{Z}_2$ orbifold has a much richer structure than many other toroidal orbifolds, in part because the moduli are not completely fixed by the orbifold quotient. In many other cases, the quotient fixes the moduli and dramatically reduces the range of possible models. Nonetheless, other models have some interesting features. For example, the $T^6/\mathbb{Z}_4 \times \mathbb{Z}_2$ orientifold has solutions with standard model-like chiral matter [33] and been used to study SU(5) GUT models [34]. Although in principle the methods of this paper could be used to study the range of models available in other orbifold constructions, in many cases the analysis is much simpler due to the absence of free moduli, and there are generally fewer distinct constructions of physical properties of interest. Two potentially interesting models for study are the $T^6/\mathbb{Z}_6$ and $T^6/\mathbb{Z}_6'$ toroidal orientifold models, which have been shown to have phenomenologically interesting solutions [35, 37]. A statistical analysis of solutions on these orbifolds has also been carried out in [36, 38]. For the $T^6/\mathbb{Z}_6'$ orientifold Gmeiner and Honecker carried out a complete analysis of solutions in [38]. They found a large total number of models, of order 10^{23}. The exponentially large number of models in this case comes from the large combinatorial number of ways in which a relatively small number of distinct branes can be combined to saturate the tadpole conditions, along with an exponential enhancement from exceptional cycles beyond those on the bulk torus. We describe in the next section how a similar feature to the first of these effects affects the distribution of complete models for the $T^6/\mathbb{Z}_2 \times \mathbb{Z}_2$ orientifold we are studying here at small integer moduli. It seems that in the

JHEP06(2009)073

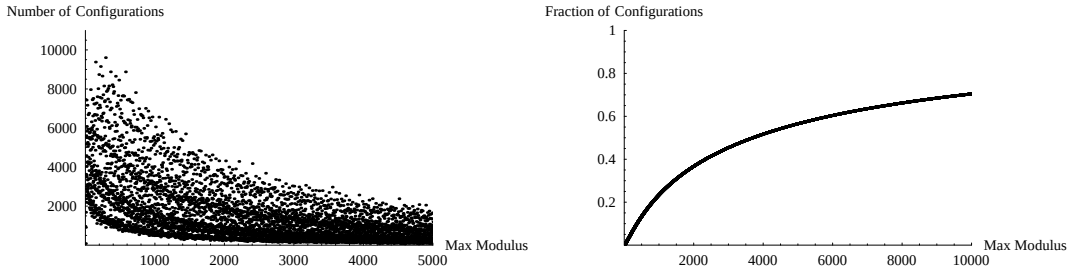

Figure 7. The upper plot shows the distribution of the number of brane configurations realizing gauge group G_{321} as a function of the maximum modulus. On the lower plot the x-axis is the maximum modulus and the y-axis is the fraction of configurations with G_{321} that have all moduli smaller than x.

$T^6/\mathbb{Z}_6'$ model, while there are many total models, the number of distinct constructions of a particular structure such as the standard model gauge group $G_{123} = \mathrm{SU}(3) \times \mathrm{SU}(2) \times \mathrm{U}(1)$ is smaller than in the $T^6/\mathbb{Z}_2 \times \mathbb{Z}_2$ case, even though the number of ways in which "extra" branes can be added to realize a complete model containing any given realization of G_{123} is large. It would be interesting to use some of the methods developed here for a further study of these and other orbifold constructions. To understand where the diversity in constructions can be found for the $T^6/\mathbb{Z}_2 \times \mathbb{Z}_2$ orientifold, it is helpful to compare our results to the analysis of Gmeiner et al. in [20], to which we now turn.

5 Diversity in the "tail" of the IBM distribution

In [20], Gmeiner, Blumenhagen, Honecker, Lüst, and Weigand undertook an ambitious computational effort to scan over all complete solutions to the tadpole, SUSY, and K-theory constraints. Their approach was to scan over the integer moduli 4-vector $\vec{U} = (h, j, k, l)$. For each set of moduli, they computed the complete set of possible brane combinations compatible with all constraints. Their analysis proceeded up to moduli with norm $|U| = 12$. Their algorithm became exponentially difficult as $|U|$ increased, but the number of solutions seemed to be decreasing for larger $|U|$, so the numerical evidence indicated that they had scanned the majority of all possible solutions, with a small fraction remaining in the tail of the distribution at larger $|U|$.

At first sight, the results of this numerical analysis seem rather at odds with the conclusions we have reached in this paper, which are that the vast majority of distinct realizations of specific gauge groups like $G_{321} = \mathrm{SU}(3) \times \mathrm{SU}(2) \times \mathrm{U}(1)$ occur in combination with **A**-branes with large negative tadpoles, which are associated with large integer moduli. To verify that most of the configurations we have found occur at large moduli, we plot in figure 7 the distribution of the maximum integer modulus ($\max(h, j, k, l) \leq |U|$) of a subset of the configurations we found that contain G_{321}. The subset for which the moduli are computed and plotted consists of those configurations in which the moduli are uniquely determined either from the realization of G_{321}, or by the branes realizing G_{321} in combination with all possible **A**-brane combinations which lead to undersaturation of

JHEP06(2009)073

the tadpole conditions. In the latter case, we use the minimum across all compatible extra **A**-brane combinations of the maximum modulus. This subset with fixed moduli represents 97% of the 13.7 million distinct realizations of G_{321}. The remaining brane configurations realizing G_{321}, not included in the plot, either do not fix the moduli at all, or require additional branes to fix the moduli for some compatible **A**-brane combinations.

The results shown in the plots in figure 7 give definitive confirmation of the story described above. Most realizations of G_{321} arise from brane configurations which fix the moduli in the range $500 < |U| < 20,000$. Less than one half of 1% of the distinct realizations of G_{321} which fix the moduli appear in the range $|U| \leq 12$ scanned in [20].

How then can these results be compatible? To understand the resolution of this apparent discrepancy it is helpful to consider the distinct nature of the questions asked in performing these two analyses. In Gmeiner et al.'s work, they were scanning over all possible brane configurations which completely saturate the tadpole constraints. Thus, at any particular value of the moduli they include all models, which for small moduli can contain a very large number of combinations of a relatively small number of distinct branes. Even if the number of combinatorial possibilities is large at small moduli, the number of distinct realizations of any particular gauge subgroup may be relatively small. On the other hand, in our analysis we are simply looking for distinct realizations of a gauge subgroup G, not necessarily counting the number of ways in which extra branes can be added to the branes forming G to form a complete model. The number of distinct realizations of G at small moduli can be relatively small, while there can be an exponentially large number of ways of completing G to a complete model. Furthermore, for more complex groups like G_{321} there may be fewer moduli at which such groups can be realized by any brane combination. Thus, the apparent discrepancy between our results and those of [20] can be understood from the realization that while the number of complete models at fixed moduli decreases fairly rapidly for small moduli, the tail of this distribution is extremely long. While the tail of the distribution may have fewer total models than the "bulk" at small moduli, it can contain a much wider diversity of realizations of any fixed gauge group G.

To check this explanation, we have considered several examples of small moduli and large moduli, and determined the total numbers of models consistent with those moduli and the tadpole and SUSY constraints. We found that indeed for small moduli, there can be many distinct solutions to the constraints. For example, for the integer moduli $(h, j, k, l) = (1, 2, 3, 4)$ there are 39,871 models coming from brane configurations which satisfy SUSY constraints and saturate the tadpole conditions (without considering K-theory constraints). For such small moduli, however, generally there are few, if any, distinct realizations of any particular group G, such as G_{321}. Those realizations of G which appear at small moduli may be consistent with many possible completions to total models through addition of different types of extra branes, but these represent a small fraction of the total number of realizations of G. At large moduli, on the other hand, generically there are few if any consistent models, with or without any particular gauge subgroup G. For example, for the moduli $(h, j, k, l) = (2, 26, 91, 1129)$ there are only 29 models in total (without considering K-theory constraints), but one of these does contain G_{321}. A clear example of the dichotomy between total number of models and numbers of distinct realizations of G

JHEP06(2009)073

is given by the simplest case, $G = \mathrm{U}(1)$. At moduli $(h, j, k, l) = (1, 2, 3, 4)$, there are 46 distinct branes, associated with 46 distinct realizations of U(1), which combine to form the 39,871 total models found there, while at moduli $(h, j, k, l) = (2, 26, 91, 1129)$, there are 14 distinct branes forming the 29 total models. Thus, while the number of total models is dramatically reduced at higher moduli, the number of distinct brane configurations realizing G does not decrease at the same rate.

Finally, as discussed in 4.5, K-theory constraints reduce the number of possible models in the tail. In [20] it was found that K-theory constraints generically reduced the number of allowed models by a factor of something like 5. At the moduli $(1, 2, 3, 4)$ discussed above, 6004 of the roughly 40,000 total models are compatible with the K-theory constraints, giving a reduction factor of around 6. At higher moduli, however, the suppression is stronger, as suggested by the discussion in section 4.5. While, for example, at the moduli (2, 26, 91, 1129) discussed above, 14 of the 29 models are compatible with K-theory (including one containing G_{321}), at other moduli containing models satisfying the tadpole and SUSY constraints there are no models at all compatible with the K-theory constraints. For example, at moduli (35, 63,1, 3455) there are 37 total models compatible with SUSY and tadpole cancellation, but none of these models satisfy the K-theory constraints. Again, the tail of the distribution is suppressed in part by the K-theory constraints, although it still seems to contain most of the diversity of models. To see how the K-theory suppression of the tail affects the distribution of configurations in the moduli space, we have checked the K-theory constraints for the **C**-brane completions of the $\mathrm{SU}(3)\times\mathrm{SU}(2)\times\mathrm{U}(1)$ configurations graphed in figure 7. Only 385,889 of these 13 million models satisfy K-theory, representing a reduction by a factor of more than 35. Of those models satisfying the K-theory constraints, roughly 90% fix all moduli. The distribution on the space of moduli is graphed in figure 8. As in the discussion of section 4.5, this represents a lower bound on the range of allowed models, as some of the configurations which do not satisfy the K-theory constraints with a pure **C**-brane completion may be compatible with K-theory constraints if **B**-branes are used in the completion to models with saturated tadpoles. Nonetheless, we expect that figure 8 presents a more accurate picture of the distribution on moduli space than figure 7. We see in figure 8 that the K-theory constraints reduce the range of brane configurations more strongly in the far end of the tail of the distribution. Nonetheless, the tail is still quite large, with many models having moduli of order 100-1000. Roughly 50% have a maximum modulus greater than 180. After imposing K-theory constraints on these models, some 5% of $\mathrm{SU}(3) \times \mathrm{SU}(2) \times \mathrm{U}(1)$ models lie within the region of moduli space scanned in [20].

Thus, while at first glance it seems that there is some apparent contradiction between the results of our analysis and those of Gmeiner et al. in [20], in fact these results are completely compatible. The reconciliation of these different analyses lies in the recognition that the distribution of models has a very long tail and there are fewer completions of a given realization of a gauge group G to a complete model in the tail. Therefore, even though the end of the tail is somewhat suppressed by the K-theory constraints, the greatest diversity of distinct realizations of specific gauge groups or matter content lies in the tail of the distribution, at large moduli.

Other large regions of the landscape which have been studied from a statistical point of view include Gepner models [39] and heterotic constructions [40]. It would be nice to

JHEP06(2009)073

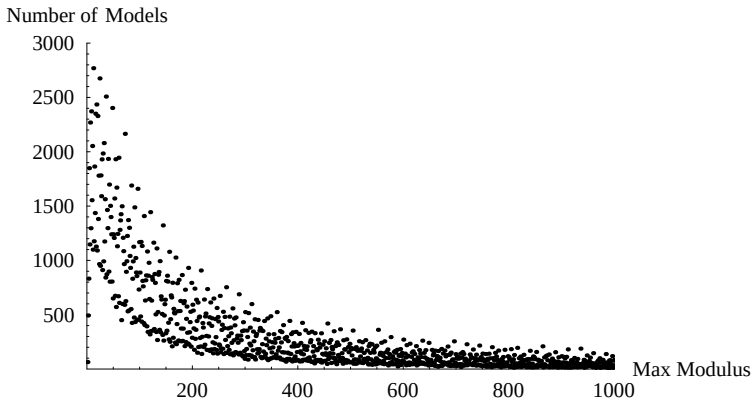

Figure 8. Distribution of a subset of models satisfying K-theory constraints. These models are formed from minimal **C**-brane completion of the configurations realizing G_{321} graphed in figure 7.

have some general lessons which are applicable to diverse sets of vacua, and the lessons learned here may have interesting ramifications for study of other patches in the landscape. From a model-building point of view, it is clearly important to understand what structure is needed to realize the greatest diversity of possible low-energy theories. From a general landscape point of view, it is important to understand how to characterize the range of low-energy physics which can be realized in a given string construction. And from the point of view of extracting general lessons from string compactifications relevant for heuristic predictions about physics beyond the standard model, the notion that the widest range of low-energy physics theories may arise in regions where there are fewer possible extensions to observable physics may have some bearing on our thinking about how string theory relates to physics which will hopefully be observed beyond the standard model. For example, it may be that in the tail of the landscape distribution, extra massive U(1) factors are not quite as ubiquitous as in the bulk of the distribution. Depending on how finely tuned our physics must be, this might decrease our expectation of seeing massive Z"s at the LHC. Or it might not. It would be rather premature to take seriously any such speculation based on our current extremely limited understanding of the nature of the full string landscape.

6 Conclusions

In this paper we have developed a systematic approach to constructing all intersecting brane models on a particular toroidal orientifold. The key technical result is the determination of all allowed combinations of branes with negative tadpole contributions, using bounds on winding numbers of these branes arising from the tadpole constraints and SUSY conditions. Given these combinations of "**A**-branes", the construction of models with any desired specific features amounts computationally to a straightforward combinatorial problem of polynomial complexity, since all other branes besides the **A**-branes must have positive tadpole contributions, and all tadpoles have a fixed bound.

JHEP06(2009)073

The methods developed here should generalize to other classes of models. For some models, such as other toroidal orientifolds [1] including the $\mathbb{Z}_6$ and $\mathbb{Z}_6'$ orbifold models studied in [36, 38], and magnetized brane models on K3 [41], there are no branes with negative tadpole contributions and/or fewer free moduli in the problem, so the problem of classifying solutions is simpler. For more general models, however, such as magnetized brane models on general Calabi-Yau manifolds, we expect an analogue of **A**-branes [21], with some negative tadpole contributions and a large number of moduli. For such models, the methods developed here may prove useful in gaining mathematical and computational control over the range of low-energy theories accessible through various brane constructions. Furthermore, the form of the mathematical problem addressed in this paper is very similar to other classes of compactification problems, such as flux compactifications, where a total tadpole constraint and SUSY conditions must be solved to determine the range of allowed constructions. It may be that some general methods similar to those developed here may be useful in addressing all of these types of vacuum classification problems.

More concretely, the analysis of this paper has given us a clear picture of the overall structure of the space of supersymmetric intersecting brane models on this particular toroidal orientifold. The computation of all combinations of branes with negative tadpoles makes possible a straightforward enumeration of all brane configurations compatible with SUSY which realize any desired gauge group and/or matter content. We have explicitly enumerated ways in which the gauge groups $\mathrm{U}(N), \mathrm{SU}(N) \times \mathrm{SU}(2) \times \mathrm{SU}(2), \mathrm{SU}(3) \times \mathrm{SU}(2)$, and $\mathrm{SU}(3) \times \mathrm{SU}(2) \times \mathrm{U}(1)$ can be realized. We found that the great majority of these gauge group realizations are associated with one or more **A**-branes with large negative tadpoles, which enables large winding numbers for the branes composing the gauge group in question, and consequent large integer moduli. The discrete K-theory constraints suppress configurations with single **A**-branes and extremely negative tadpoles.

We have found that the greatest diversity in realizations of any given gauge group and matter structure occurs in the "tail" of the distribution of models. This tail is characterized by large integer moduli, generally outside the range encompassed by the systematic scan of [20], and by one, or sometimes several D-branes of type **A** with a very negative tadpole. In this tail, at fixed moduli, the number of ways in which a given realization of a small gauge group can be completed to form the total gauge group is much smaller than in the "bulk" of the distribution at small moduli, where there are many possible configurations of extra brane sectors, which could be hidden or, more usually, include additional chiral matter fields charged under the desired gauge group. We have found evidence for further suppression of the tail from the K-theory constraints. Nonetheless, the vast majority of distinct realizations of any given small gauge group occur in the tail of the distribution, at large moduli. It is difficult to make concrete statements about the larger string landscape based on this one sample, but it seems plausible that this feature of "diversity in the tail" of the distribution may be valid in more general classes of compactifications. If so, this might give some insight both into efficient strategies for realistic model-building, and into the expected range of additional gauge group and matter content (such as the number of Z"s) which may arise naturally from string theory in generic extensions of the standard model. It would be interesting to understand the phenomenon discovered here of diversity

JHEP06(2009)073

in the tail of the landscape distribution in terms of some more general measure on the moduli space, along the lines of [42]. Understanding more generally where the diversity of low-energy physics arises in the distribution of models on the landscape may lead to a useful refinement of the statistical approach to the string landscape pioneered by Douglas in [43].

Another general lesson of the results in this paper is that what appear to be "typical" features of a model depend strongly on the prior assumptions made about the structure of the model. If several assumptions are made, each associated with a cut on the data, then depending on the form of these assumptions, conclusions may depend upon the order in which the cuts are made. For example, if one first makes the assumption that one is interested in a "typical" model in the space of all consistent intersecting brane models on the $T^6/\mathbb{Z}_2 \times \mathbb{Z}_2$ orientifold, and therefore restricts to models with small moduli, and second makes the assumption that the gauge group contains $G_{321} = \mathrm{SU}(3) \times \mathrm{SU}(2) \times \mathrm{U}(1)$, then one reaches a much more restrictive set of possible models then if one first makes the assumption that the gauge group contains G_{321}, and then looks for typical features among the 16 million or so distinct realizations of G_{321}. In particular, as the analysis of this paper shows, the order of cuts in this case impacts the number of possible "hidden sectors" which can complete the model with gauge group G_{321} to form a complete and consistent intersecting brane model satisfying the tadpole and supersymmetry constraints. These results suggest that model-building by "trial and error" may be less productive in generating models with interesting phenomenology than more systematic searches which hone in on subsets of models with desired features which may be found in atypical places in the parameter space of models. This lesson may be useful to keep in mind in other contexts involving analysis of regions of the string landscape.

Acknowledgments

It is a pleasure to thank Allan Adams, Ralph Blumenhagen, Mirjam Cvetič, Michael Douglas, Florian Gmeiner, Gabriele Honecker, Vijay Kumar, Dieter Lüst, John McGreevy, Robert Richter, Gary Shiu, and Timo Weigand for helpful discussions and comments. Particular thanks to Michael Douglas for collaboration on the work reported in [21] and further discussions which helped initiate this work. Particular thanks also to Gabriele Honecker and Robert Richter for detailed comments on a preliminary version of this manuscript. Thanks also to the KITP for support and hospitality while part of this work was being completed. This research was supported by the DOE under contract #DE-FC02-94ER40818. This research was also supported in part by the National Science Foundation under Grant No. PHY05-51164.

A Configurations of A-branes with 4 distinct negative tadpoles

In this appendix we show there are no **A**-brane configurations with 4 different negative tadpoles ($[p, q, r, s]$) when the tadpole constraint has $T = 8$. We use the notation introduced in section 3 and recall that the branes can be arranged so that the p branes with the negative

JHEP06(2009)073

P tadpole are first in the configuration, followed by the q branes with a negative Q tadpole, then r branes with a negative R, and finally s branes with a negative S. Additionally, within these groupings the negative tadpoles are ordered in increasing order of their absolute value. We write all tadpbole numbers as the absolute value of the tadpole contribution and explicity insert the minus sign. So, for instance we have that $P_1 \leq P_2 \leq \ldots \leq P_p$ and similarly for Q, R, and S tadpoles. Furthermore, for convenience of notation, we let $a = p,\ b = p+q,\ c = p+q+r,\ d = p+q+r+s$ and without loss of generality, $p \geq q \geq r \geq s$.

Let us look at branes b, c, and d. Since there are $p+r+s-2$ branes other than branes c and d with a tadpole other than Q that is negative, and since Q_b is the largest of the negative Q tadpoles, the tadpole constraint gives

$$Q_c + Q_d \leq 8 + qQ_b - (p+r+s-2). \tag{A.1}$$

Using the identity $\frac{1}{x} + \frac{1}{y} \geq \frac{4}{x+y}$ we have that

$$\frac{1}{Q_c} + \frac{1}{Q_d} \geq \frac{4}{10 + qQ_b - (p+r+s)}. \tag{A.2}$$

Looking at branes a, b, c, d and using the tadpole constraint

$$Q_a + Q_c + Q_d \leq 8 + qQ_b - (p+r+s-3) \tag{A.3}$$

we similarly get

$$\frac{1}{Q_a} + \frac{1}{Q_c} + \frac{1}{Q_d} \geq \frac{9}{11 + qQ_b - (p+r+s)}. \tag{A.4}$$

The analogous relation for the P's gives

$$\frac{1}{P_b} + \frac{1}{P_c} + \frac{1}{P_d} \geq \frac{9}{11 + pP_a - (q+r+s)}. \tag{A.5}$$

Recalling 3.9 which states

$$p + q \leq 7, \tag{A.6}$$

combined with the assumption $p \geq q \geq r \geq s$, gives

$$p + r + s \leq 10. \tag{A.7}$$

We are now going to show there are no solutions for the following three cases:

a) $p \leq q + r + s - 2$

b) $q \leq p + r + s - 6$

c) $q = r = s = 1$

a) Using $P_a \geq 1$ combined with the assumption $p \leq q + r + s - 2$ we get $(9-p)P_a \geq 11 - (q+r+s)$. Rearranging gives $9P_a \geq 11 - (q+r+s) + pP_a$. Using (A.7) along

with $p \geq q$ shows us that $11-(q+r+s) > 0$. Therefore the right side of (A.5) is greater than or equal to $1/P_a$,

$$\frac{9}{11+pP_a-(q+r+s)} \geq \frac{9}{9P_a} = \frac{1}{P_a}. \tag{A.8}$$

So using (A.5) we see that the sum of the inverses of the Ps for branes a, b, c and d is greater than or equal to 0

$$-\frac{1}{P_a}+\frac{1}{P_b}+\frac{1}{P_c}+\frac{1}{P_d} \geq 0. \tag{A.9}$$

Analogous arguments show that the sum of the inverses of the $Q's$ for these 4 branes is greater than or equal to 0, as is the sum of the inverses of the $R's$ and $S's$. If we now add the SUSY equations (2.8) for branes a, b, c and d, the right side is 0 while the left side is greater than or equal to 0. For there to be equality, (A.9) and (A.8) must be equalities, requiring $(9-p)P_a = 11-(q+r+s)$. This means $P_a = 1$ and $p+2 = q+r+s$, implying (using (A.6)) that $r = s = 1$. The analogous equations to (A.9) for the $Q's, R's$ and $S's$ must also be equalities and thus $P_a = Q_b = R_c = S_d = 1$ and $p = q = r = s = 1$. The SUSY and tadpole constraints prevent this from occuring. Hence, there are no solutions in case (a).

b) Using $Q_b \geq 1$ combined with (A.7) we get for the right side of (A.2)

$$\frac{4}{10+qQ_b-(p+r+s)} \geq \frac{4}{10+q-(p+r+s)}\frac{1}{Q_b}. \tag{A.10}$$

By assumption $10+q-(p+r+s) \leq 4$. Thus with use of (A.2) we get

$$-\frac{1}{Q_b}+\frac{1}{Q_c}+\frac{1}{Q_d} \geq 0. \tag{A.11}$$

Similarly the sum of the inverses of the $R's$ and $S's$ from branes b, c, and d are greater than or equal to 0. Adding the SUSY equations (2.8) from branes b, c and d we see there are no solutions in case (b).

c) We begin with the case of $[2, 1, 1, 1]$. Using (A.4) we see that $\frac{1}{Q_2}-\frac{1}{Q_3}+\frac{1}{Q_4}+\frac{1}{Q_5} > 0$. Similarly the sum of the inverses of the $R's$ and $S's$ for the last 4 branes is greater than 0. Upon adding the SUSY equations for these four branes we see that we must have $-\frac{1}{P_2}+\frac{1}{P_3}+\frac{1}{P_4}+\frac{1}{P_5} < 0$. Applying (A.5) this means $\frac{9}{11+2P_2-3} < \frac{1}{P_2}$. Rearranging shows $P_2 < 8/7$. Combined with the assumption that $P_1 \leq P_2$ gives $P_1 = P_2 = 1$. From (A.2) we get $\frac{1}{Q_4}+\frac{1}{Q_5} \geq \frac{4}{7}\frac{1}{Q_3}$. Similarly, $\frac{1}{S_3}+\frac{1}{S_4} \geq \frac{4}{7}\frac{1}{S_5}$ and $\frac{1}{R_3}+\frac{1}{R_5} \geq \frac{4}{7}\frac{1}{R_4}$. Now adding the SUSY equations for the last three branes we find that

$$\frac{1}{P_3}+\frac{1}{P_4}+\frac{1}{P_5} \leq \frac{3}{7}\left(\frac{j}{Q_3}+\frac{k}{R_4}+\frac{l}{S_5}\right). \tag{A.12}$$

Using similar arguments to those used to derive (A.4) (and the discrete nature of the integers) we get

$$\frac{1}{Q_1}+\frac{1}{Q_2}+\frac{1}{Q_4}+\frac{1}{Q_5}\geq\frac{11}{6}\frac{1}{Q_3}.$$

Note that equality for this equation occurs at, for example, $Q_1=3$ and $Q_2=Q_4=Q_5=2$. The analogous equations hold for the $R's$ and $S's$. Now we add the SUSY equations for all 5 branes and remember that $P_1=P_2=1$. This gives

$$2-\left(\frac{1}{P_3}+\frac{1}{P_4}+\frac{1}{P_5}\right)\geq\frac{5}{6}\left(\frac{j}{Q_3}+\frac{k}{R_4}+\frac{l}{S_5}\right) \tag{A.13}$$

Combining the two inequalities (A.12) and (A.13), we find that $\frac{1}{P_3}+\frac{1}{P_4}+\frac{1}{P_5}\leq\frac{36}{53}$. Subject to the tadpole condition $P_3+P_4+P_5\leq 10$, this has no solutions.

For $p=3$ and $p=4$ we can use an analogous argument to the one above. For $p\geq 5$ we notice that $-\frac{1}{Q_{a+1}}+\frac{1}{Q_{a+2}}+\frac{1}{Q_{a+3}}>0$ and similarly for the Rs and Ss. Adding the SUSY equations for the last 3 branes, we see that there can be no solutions.

There are only 5 remaining cases not included in $a-c$. They are $[3,2,1,1]$, $[4,2,1,1]$, $[5,2,1,1]$, $[4,3,1,1]$, and $[4,2,2,1]$. Using (A.4) and (A.5) in analogous way as before, for all of them we find $P_a=1$. Use of FWNB (3.1) and TCSB (3.5) imposes tight constraints on the other tadpoles, allowing for a systematic search which reveals there are no solutions in any of these cases.

References

[1] R. Blumenhagen, L. Görlich and B. Körs, *Supersymmetric orientifolds in 6D with D-branes at angles*, *Nucl. Phys.* **B 569** (2000) 209 [hep-th/9908130] [SPIRES]; *Supersymmetric 4D orientifolds of type IIA with D6-branes at angles*, *JHEP* **01** (2000) 040 [hep-th/9912204] [SPIRES]; *A new class of supersymmetric orientifolds with D-branes at angles*, hep-th/0002146 [SPIRES];
R. Blumenhagen, L. Görlich, B. Körs and D. Lüst, *Noncommutative compactifications of type-I strings on tori with magnetic background flux*, *JHEP* **10** (2000) 006 [hep-th/0007024] [SPIRES];
C. Angelantonj, I. Antoniadis, E. Dudas and A. Sagnotti, *Type-I strings on magnetised orbifolds and brane transmutation*, *Phys. Lett.* **B 489** (2000) 223 [hep-th/0007090] [SPIRES];
G. Aldazabal, S. Franco, L.E. Ibáñez, R. Rabadán and A.M. Uranga, *Intersecting brane worlds*, *JHEP* **02** (2001) 047 [hep-ph/0011132] [SPIRES].

[2] C. Bachas, *A way to break supersymmetry*, hep-th/9503030 [SPIRES].

[3] M. Berkooz, M.R. Douglas and R.G. Leigh, *Branes intersecting at angles*, *Nucl. Phys.* **B 480** (1996) 265 [hep-th/9606139] [SPIRES].

[4] A.M. Uranga, *Chiral four-dimensional string compactifications with intersecting D-branes*, *Class. Quant. Grav.* **20** (2003) S373 [hep-th/0301032] [SPIRES].

[5] E. Kiritsis, *D-branes in standard model building, gravity and cosmology*, *Fortsch. Phys.* **52** (2004) 200 [hep-th/0310001] [SPIRES].

JHEP06(2009)073

[6] D. Lüst, *Intersecting brane worlds: a path to the standard model?*, *Class. Quant. Grav.* **21** (2004) S1399 [hep-th/0401156] [SPIRES].

[7] R. Blumenhagen, M. Cvetič, P. Langacker and G. Shiu, *Toward realistic intersecting D-brane models*, *Ann. Rev. Nucl. Part. Sci.* **55** (2005) 71 [hep-th/0502005] [SPIRES].

[8] R. Blumenhagen, B. Körs, D. Lüst and S. Stieberger, *Four-dimensional string compactifications with D-branes, orientifolds and fluxes*, *Phys. Rept.* **445** (2007) 1 [hep-th/0610327] [SPIRES].

[9] F. Marchesano, *Progress in D-brane model building*, *Fortsch. Phys.* **55** (2007) 491 [hep-th/0702094] [SPIRES].

[10] D. Lüst, *Seeing through the string landscape — A string hunter's companion in particle physics and cosmology*, *JHEP* **03** (2009) 149 [arXiv:0904.4601] [SPIRES].

[11] R. Blumenhagen, M. Cvetič, S. Kachru and T. Weigand, *D-brane instantons in type II string theory*, arXiv:0902.3251 [SPIRES].

[12] S. Förste, G. Honecker and R. Schreyer, *Supersymmetric $Z(N) \times Z(M)$ orientifolds in 4D with D- branes at angles*, *Nucl. Phys.* **B 593** (2001) 127 [hep-th/0008250] [SPIRES].

[13] M. Cvetič, G. Shiu and A.M. Uranga, *Three-family supersymmetric standard like models from intersecting brane worlds*, *Phys. Rev. Lett.* **87** (2001) 201801 [hep-th/0107143] [SPIRES].

[14] M. Cvetič, G. Shiu and A.M. Uranga, *Chiral four-dimensional $N = 1$ supersymmetric type IIA orientifolds from intersecting D6-branes*, *Nucl. Phys.* **B 615** (2001) 3 [hep-th/0107166] [SPIRES].

[15] D. Cremades, L.E. Ibáñez and F. Marchesano, *Yukawa couplings in intersecting D-brane models*, *JHEP* **07** (2003) 038 [hep-th/0302105] [SPIRES].

[16] M. Cvetič, P. Langacker, T.-J. Li and T. Liu, *D6-brane splitting on type IIA orientifolds*, *Nucl. Phys.* **B 709** (2005) 241 [hep-th/0407178] [SPIRES].

[17] F. Marchesano and G. Shiu, *MSSM vacua from flux compactifications*, *Phys. Rev.* **D 71** (2005) 011701 [hep-th/0408059] [SPIRES].

[18] M. Cvetič, T. Li and T. Liu, *Supersymmetric Pati-Salam models from intersecting D6-branes: a road to the standard model*, *Nucl. Phys.* **B 698** (2004) 163 [hep-th/0403061] [SPIRES].

[19] R. Blumenhagen, F. Gmeiner, G. Honecker, D. Lüst and T. Weigand, *The statistics of supersymmetric D-brane models*, *Nucl. Phys.* **B 713** (2005) 83 [hep-th/0411173] [SPIRES].

[20] F. Gmeiner, R. Blumenhagen, G. Honecker, D. Lüst and T. Weigand, *One in a billion: MSSM-like D-brane statistics*, *JHEP* **01** (2006) 004 [hep-th/0510170] [SPIRES].

[21] M.R. Douglas and W. Taylor, *The landscape of intersecting brane models*, *JHEP* **01** (2007) 031 [hep-th/0606109] [SPIRES].

[22] A.M. Uranga, *D-brane probes, RR tadpole cancellation and k-theory charge*, *Nucl. Phys.* **B 598** (2001) 225 [hep-th/0011048] [SPIRES].

[23] K.R. Dienes and M. Lennek, *Fighting the floating correlations: expectations and complications in extracting statistical correlations from the string theory landscape*, *Phys. Rev.* **D 75** (2007) 026008 [hep-th/0610319] [SPIRES].

[24] G. Aldazabal, S. Franco, L.E. Ibáñez, R. Rabadán and A.M. Uranga, *$D = 4$ chiral string compactifications from intersecting branes*, *J. Math. Phys.* **42** (2001) 3103 [hep-th/0011073] [SPIRES].

JHEP06(2009)073

[25] L.E. Ibáñez, F. Marchesano and R. Rabadán, *Getting just the standard model at intersecting branes*, *JHEP* **11** (2001) 002 [hep-th/0105155] [SPIRES].

[26] F. Gmeiner and M. Stein, *Statistics of* SU(5) *D-brane models on a type-II orientifold*, *Phys. Rev.* **D 73** (2006) 126008 [hep-th/0603019] [SPIRES].

[27] F.G. Marchesano Buznego, *Intersecting D-brane models*, hep-th/0307252 [SPIRES].

[28] M. Cvetič, I. Papadimitriou and G. Shiu, *Supersymmetric three family* SU(5) *grand unified models from type IIA orientifolds with intersecting D6-branes*, *Nucl. Phys.* **B 659** (2003) 193 [*Erratum ibid.* **B 696** (2004) 298] [hep-th/0212177] [SPIRES].

[29] J. Kumar and J.D. Wells, *Landscape cartography: a coarse survey of gauge group rank and stabilization of the proton*, *Phys. Rev.* **D 71** (2005) 026009 [hep-th/0409218] [SPIRES]; *Surveying standard model flux vacua on* $T^6/\mathbb{Z}_2 \times Z(2)$, *JHEP* **09** (2005) 067 [hep-th/0506252] [SPIRES].

[30] F. Marchesano and G. Shiu, *Building MSSM flux vacua*, *JHEP* **11** (2004) 041 [hep-th/0409132] [SPIRES].

[31] M. Cvetič, T. Li and T. Liu, *Standard-like models as type IIB flux vacua*, *Phys. Rev.* **D 71** (2005) 106008 [hep-th/0501041] [SPIRES].

[32] M.P. Hertzberg, S. Kachru, W. Taylor and M. Tegmark, *Inflationary constraints on type IIA string theory*, *JHEP* **12** (2007) 095 [arXiv:0711.2512] [SPIRES].

[33] G. Honecker, *Chiral supersymmetric models on an orientifold of* $Z(4) \times Z(2)$ *with intersecting D6-branes*, *Nucl. Phys.* **B 666** (2003) 175 [hep-th/0303015] [SPIRES].

[34] M. Cvetič and P. Langacker, *New grand unified models with intersecting D6-branes, neutrino masses and flipped* SU(5), *Nucl. Phys.* **B 776** (2007) 118 [hep-th/0607238] [SPIRES].

[35] G. Honecker and T. Ott, *Getting just the supersymmetric standard model at intersecting branes on the Z(6)-orientifold*, *Phys. Rev.* **D 70** (2004) 126010 [*Erratum ibid.* **D 71** (2005) 069902] [hep-th/0404055] [SPIRES].

[36] F. Gmeiner, D. Lüst and M. Stein, *Statistics of intersecting D-brane models on* T^6/Z_6, *JHEP* **05** (2007) 018 [hep-th/0703011] [SPIRES].

[37] D. Bailin and A. Love, *Towards the supersymmetric standard model from intersecting D6-branes on the* $Z'(6)$ *orientifold*, *Nucl. Phys.* **B 755** (2006) 79 [*Nucl. Phys.* **B 783** (2007) 176] [hep-th/0603172] [SPIRES]; *Almost the supersymmetric standard model from intersecting D6-branes on the* $Z'(6)$ *orientifold*, *Phys. Lett.* **B 651** (2007) 324 [*Erratum ibid.* **B 658** (2008) 292] [arXiv:0705.0646] [SPIRES].

[38] F. Gmeiner and G. Honecker, *Mapping an island in the landscape*, *JHEP* **09** (2007) 128 [arXiv:0708.2285] [SPIRES]; *Millions of standard models on* $Z(6)'$*?*, *JHEP* **07** (2008) 052 [arXiv:0806.3039] [SPIRES].

[39] T.P.T. Dijkstra, L.R. Huiszoon and A.N. Schellekens, *Supersymmetric standard model spectra from RCFT orientifolds*, *Nucl. Phys.* **B 710** (2005) 3 [hep-th/0411129] [SPIRES]; P. Anastasopoulos, T.P.T. Dijkstra, E. Kiritsis and A.N. Schellekens, *Orientifolds, hypercharge embeddings and the standard model*, *Nucl. Phys.* **B 759** (2006) 83 [hep-th/0605226] [SPIRES].

JHEP06(2009)073

[40] K.R. Dienes, *Statistics on the heterotic landscape: gauge groups and cosmological constants of four-dimensional heterotic strings*, *Phys. Rev.* **D 73** (2006) 106010 [hep-th/0602286] [SPIRES].

[41] V. Kumar and W. Taylor, *Freedom and constraints in the $K3$ landscape*, *JHEP* **05** (2009) 066 [arXiv:0903.0386] [SPIRES].

[42] S. Ashok and M.R. Douglas, *Counting flux vacua*, *JHEP* **01** (2004) 060 [hep-th/0307049] [SPIRES].

[43] M.R. Douglas, *The statistics of string/M theory vacua*, *JHEP* **05** (2003) 046 [hep-th/0303194] [SPIRES].

JHEP06(2009)073